J. Webster (ed.), *Wiley Encyclopedia of Electrical and Electronics Engineering*


# OSCILLATOR DESIGN

The development of electronic oscillators was strongly related to the invention of the vacuum tube at the beginning of the twentieth century. The first oscillator circuits were presented by Meissner, Hartley, and Colpitts, among others, and basic ideas for a theory of such circuits were presented by Vallauri in 1917 (1). In 1914 Zenneck considered an oscillatory arrangement with an arc as the active device, and he discussed nonlinear aspects of electronic oscillators by means of an energy balance equation. Unfortunately, he did not derive the corresponding differential equations for the currents and voltages. A differential equation for a triode oscillator was presented for the first time by van der Pol in 1920. His studies became the starting point for a long series of research in mathematics, physics, and electrical engineering on oscillatory networks and systems. As a result, a first monumental monograph about this subject was published by Andronov et al. in 1937 (2) that included the essential aspects of the theory of oscillatory circuits and systems and was illustrated by many examples. At the same time Krylov and Bogoliubov (3) published essential results about the analysis of oscillatory circuits. Both groups started from the work of van der Pol and used ideas and results from the work of the French mathematician and physicist Henri Poincaré. Short presentations of the history of these methods can be found in Sanders and Verhulst (4) and Mathis (5). Although the results of these authors were discussed several times in the literature, most of them were unknown to many researchers until the late sixties. Maybe this is one of the reasons that, in contrast to the linear analysis of oscillatory circuits and systems, details of the nonlinear theory due to the above-mentioned Russian research groups were not included in a design theory of oscillators. We will show in this article that the design of oscillators can be clarified if their ideas are included.

## Foundations

**Properties of Electrical Oscillators.** In order to understand the difficulties related to electronic oscillators it is useful to discuss the main properties of the behavior of such electronic circuits and consider some aspects of their modelling. It is well known that the basic behavior of an electronic oscillator should be characterized as follows (e.g. Parzen (6)]:

- Some voltages and/or currents should behave in a periodic manner. The most important shapes of the output are sinusoidal, saw tooth, and square waves.
- The oscillator frequency should be well determined.
- After a transient, the oscillator amplitude should be well determined and independent of the initial conditions.
- Perturbations of the oscillatory behavior in the steady state should die out after some transient behavior.
- The oscillatory behavior should not be destroyed by parasitic circuit elements (structural stability).

From these qualitative properties the main features of electronic oscillators can be extracted and serve as main specifications:

- Oscillator frequency
- Oscillator amplitude
- Rate of the startup and decay

Obviously we have to add further properties if electronic oscillators are to be designed. The signal-to-noise ratio, the stability of the oscillator frequency and amplitude and the distortions with respect to a desired waveform are a few of these properties. The basic behavior of electronic oscillators cannot be realized or modelled by using linear (time-invariant) circuits, because such circuits have to be nondissipative (no ohmic resistors can be included) if periodic behavior is desired. Therefore, the energy is conserved and their oscillatory amplitude depends on the initial conditions. Furthermore, such linear (nondissipative) oscillator models are not structurally stable (see the above characterization), because the periodic behavior is destroyed by arbitrarily small dissipative elements (e.g. ohmic resistors). Thus mathematical models of electronic oscillators have to be nonlinear. In 1963 it was emphasized by Hale (7) that our knowledge of nonlinear systems is still far from complete, and only a few mathematical techniques are available to analyze such models. Although intensive research has been carried out in this area for more than thirty years, many problems still have to be solved to obtain a satisfactory theory. Good illustrations of this statement can be found in Guckenheimer's discussion of the van der Pol equation (8).

**Oscillator Models.** Although a linear $LC$-circuit without dissipation is not suitable as a complete model for electronic oscillators, it is useful to start with such a circuit and to introduce the following changes:

- Compensation of the dissipation with negative resistors or positive feedback
- Comparison of the oscillator amplitude with a prescribed value in an implicit or explicit manner, and control the negative resistor or the feedback

It should be emphasized that compensation is a linear technique, whereas amplitude control by using parameter variation is an inherently nonlinear technique.

These two steps can be described mathematically if we start from the differential equation for an $LC$ circuit with a rather small resistor (dissipation).

$$\ddot{x} + \gamma \dot{x} + \omega_0^2 x = 0 \qquad (1)$$

where $\gamma$ is proportional to the (positive) resistance. Using a compensation technique, $\gamma$ can be cancelled. For example, this can be done by adding a negative resistor in series (or parallel) with the positive resistor, with the same magnitude. If Eq. (1) is converted to the state-space form $\dot{\boldsymbol{x}} = \boldsymbol{A}\boldsymbol{x}$ by the notation $x_1 := x$, $x_2 := \dot{x}$, it is easy to see that applying a compensation technique results in a pair of eigenvalues of $A$ on the imaginary axis. In more general cases the state space has dimension $n > 2$, since there are more than two reactances. Usually the matrix $A$ has at least one pair of eigenvalues other than those with negative real parts. In the subsection "The Linear Design Theory of Sinusoidal Oscillators" below, several approaches are discussed that can be used to find a set of parameters where a pair of eigenvalues with zero real part occur. Furthermore, it should be emphasized that it is not necessary that we start with an $LC$ circuit, since it is for example, possible, to realize inductors in an active manner by means of resistors, capacitors, and (operational) amplifiers. In contrast to $LC$ oscillators, these kind of oscillators are called $RC$ oscillators [see e.g. Millman and Grabel (9)]. The first $RC$ oscillator was presented by Heegner (10) in 1927; see also Sidorowicz (11) further references.

If the resistor, or in other words $\gamma$, is controlled by the state variables $(x, \dot{x})$, we get the following nonlinear differential equation:

$$\ddot{x} + \gamma(x, \dot{x})\dot{x} + \omega_0^2 x = 0 \qquad (2)$$

Special choices of the function $\gamma = \gamma(x, \dot{x})$ lead to particular nonlinear oscillator models. In the next subsection this problem is discussed by means of the theorem of Poincaré, Andronov and Hopf.

It is mentioned above that the van der Pol (*vdP*) equation was the first model of an oscillator circuit. The normalized version of this equation has the following form (with normalized ${\omega^2}_0 = 1$):

$$\ddot{x} + \varepsilon(x^2 - 1)\dot{x} + x = 0 \tag{3}$$

Note that this differential equation is of the above-mentioned form. Another differential equation of a similar type is the (R) Rayleigh equation (with normalized ${\omega^2}_0 = 1$)

$$\ddot{x} + \varepsilon(\dot{x}^2 - 1)\dot{x} + x = 0 \tag{4}$$

Unfortunately, the equilibrium solution $O := \{x(t) = 0 \mid t \; \varepsilon \; IR\}$ is the only solution that is known in exact terms. All other solutions, and in particular the periodic solution, have to be calculated with perturbation methods. Therefore we consider a modified differential equation (with normalized ${\omega^2}_0 = 1$),

$$\ddot{x} + \varepsilon(x^2 + \dot{x}^2 - 1)\dot{x} + x = 0 \tag{5}$$

with the periodic solution $x_\mathrm{p} := \{\mathrm{x(t)} = \cos t \; t \; \varepsilon \; IR\}$, which can be calculated in a simple manner. Obviously, this solution is unique up to an additive phase $\varphi$, and the periodic solution does not depend on the parameter $\epsilon$. An advantage of this equation is that it can be interpreted very easily. For this reason $x_\mathrm{p}$ is represented in the state space ($x_1 := \dot{x}$, $x_2 := x$) as a circle. The state-space representation of Eq. (5) is

$$\dot{x}_1 = -x_2 - \varepsilon(x_1^2 + x_2^2 - 1)x_1 \tag{6}$$

$$\dot{x}_2 = x_1 \tag{7}$$

Within the circle the (nonlinear) coefficient of the second term in Eq. (5) is negative, and outside the circle the coefficient is positive. If this coefficient is constant, both differential equations correspond to the descriptive equation of an *LC* circuit with linear damping through an ohmic resistor. If we assume the (nonlinear) coefficient in Eq. (5) to be constant for a moment, the first case corresponds to an *LC* circuit with a negative resistor, and the second case to a circuit with a positive resistor. From this heuristic point of view it is easy to interpret the global behavior of Eq. (5). Although its solutions cannot be calculated analytically if the initial conditions are prescribed within or outside the circle $x_\mathrm{p}$, the qualitative behavior of the differential equation follows from the analogy with an *LC* circuit with damping. We find that the amplitude of every solution that starts within the circle increases and approaches $x_\mathrm{p}$ as $t \to \infty$. On the other hand, the amplitude of every solution that starts outside the circle decreases and approaches $x_\mathrm{p}$ as $t \to \infty$. From a physical point of view the two-dimensional state space of the differential equation (5) is decomposed by the circle $x_\mathrm{p}$ into two areas that have different meanings:

- The negative-damping area (inside the circle), where energy is supplied to the system
- The positive-damping areas (outside the circle) where energy is dissipated by the system.

The periodic solution $x_\mathrm{p}$ can be interpreted as a dynamical equilibrium between the negative and the positive damping area. Stable periodic solutions of this kind are called limit cycles [see e.g. Jordan and Smith

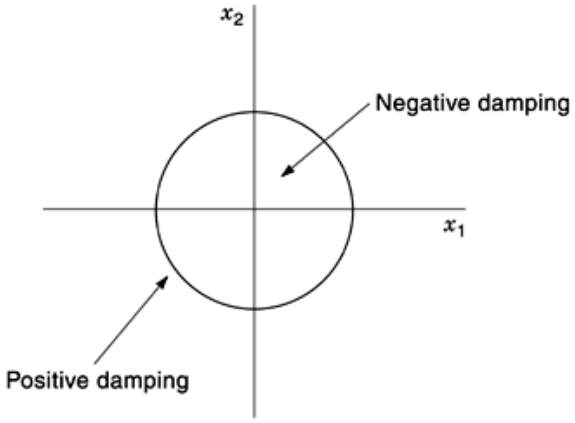


**Fig. 1.** Negative-damping area of the Rayleigh–van der Pol equation.

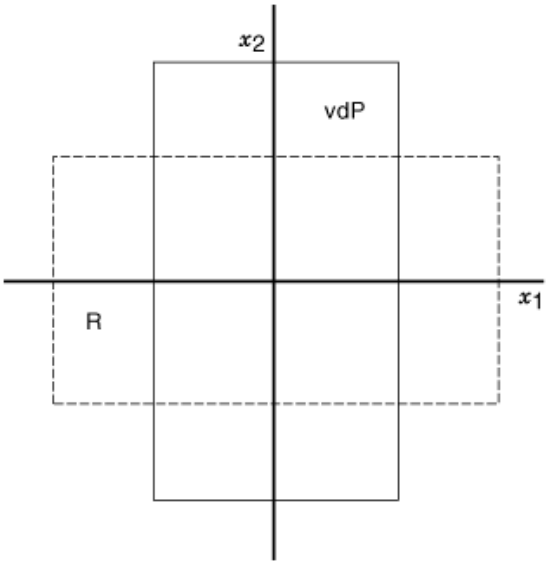


**Fig. 2.** Damping areas: vdP van der Pol equation; R Rayleigh Equation.

(12)]. In contrast to limit cycles, a stable equilibrium $O$ is embedded in a positive-damping area. Both types of solutions are called steady-state solutions. In Fig. 1 the state space and the steady-state solutions of Eq. (5) are shown together with the damping area.

The physical situation of this rather special differential equation is the typical case in two-dimensional state-space systems. In Fig. 2 we show the damping areas of the van der Pol equation and of the Rayleigh equation, which extend infinitely in the $x_2$ and $x_1$ directions, respectively. It is clear why sinusoidal solutions are impossible, since the damping areas are not symmetric with respect to the unstable zero solution point.

The parameter $\epsilon$ can be interpreted as a measure of deviation from the sinusoidal case. If $\varepsilon << 1$, we have a sinusoidal oscillator that is discussed in the next sections. For large $\epsilon >> 1$ we obtain a relaxation oscillator that is considered in this subsection. The latter case is much more complicated from a mathematical point of view, because circuits of this kind have to be described by differential–algebraic equations or analyzed

by singular perturbation methods [see e.g. Mathis (5)]. However, the design of square-wave oscillators can be simplified if the transistors are modelled as switches. Such models are piecewise linear. In the case of sinusoidal oscillators an overall model is available.

**The Mandelstam–Papalexi–Andronov Oscillator Model.** Although the simple oscillator equations in the last section are very suitable for illustrating the physical reason for periodic steady-state solutions, a more extended model should be considered that includes additional parameters. From a systematic point of view a family of differential equations is considered that is parametrized by means of the mentioned parameter, and the following questions are studied:

- Is there a subset of equations that permit a periodic steady-state solution?
- If so, what is the critical value of the parameter where a qualitative change within the family arises?

These questions are crucial for the design of electronic oscillator circuits. Therefore these problems were studied around 1930 by Mandelstam, Papalexi, and Andronov using ideas from Poincare's theory of celestrial mechanics. As a result they proved a theorem including a criterion for the occurrence of a limit cycle in differential equations depending on a certain parameter. In the mathematical literature this theorem is known as the Hopf bifurcation theorem because Hopf, rediscovered it in 1944 while studying problems in hydromechanics [see Arnold (13)], p. 271) for further information about the reception of this theorem]. The Mandelstam–Papalexi–Andronov oscillator model contains a parameter that is suitable for generating a limit cycle if a critical value is passed. In oscillator design this parameter corresponds to a circuit parameter. (e.g. the load resistor). Before formulating the Poincaré–Andronov–Hopf theorem, we will demonstrate the birth of a limit cycle. For this purpose a modification of Eq. (5) is used, since it can be solved exactly. This equation is formulated in the state-space representation [see e.g. Nicolis and Prigogine (14)]

$$\dot{x}_1 = -x_2 - (x_1^2 + x_2^2 - \mu)x_1 \tag{8}$$

$$\dot{x}_2 = x_1 - (x_1^2 + x_2^2 - \mu)x_2 \tag{9}$$

where the parameter is included in another way. To solve this differential equation we transform it into the magnitude–phase–angle representation

$$\dot{r} = \mu r - r^3 \tag{10}$$

$$\dot{\varphi} = 1 \tag{11}$$

Obviously the system of two differential equations is decoupled, and in this case solutions of both equations are known. We have

$$r = r(t) = \sqrt{|\mu|}\frac{\exp \mu t}{\sqrt{1 + \exp 2\mu t}} \quad \text{and} \quad \varphi = \varphi(t) = \varphi_0 + t \tag{12}$$

In Fig. 3 the steady-state behavior of Eqs. (8), (9) is illustrated for $\mu < 0$ and $\mu > 0$, and we find that in the latter case we have the desired limit cycle. The above-mentioned critical parameter value is zero.

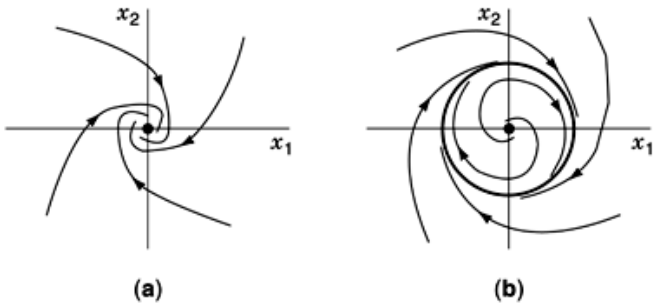


**Fig. 3.** Bifurcation of a limit Cycle: (a) $\mu < 0$, (b) $\mu > 0$.

It can be shown that this case already describes a very general situation. If we consider $n$-dimensional systems of differential equations that describe more complicated electronic oscillators, the so-called center manifold theorem can be used to reduce the dimension of the system to two. [For details of this theorem we refer to the monograph of Arrowsmith and Place. (15)]. Then the former case is obtained, but in this introductory article we cannot discuss further details, and therefore the reader is referred, (for example) to Hassard et al. (16).

In the following, the Poincaré–Andronov–Hopf theorem is formulated.

Theorem (Poincaré–Andronov–Hopf). Let

$$\dot{\boldsymbol{x}} = \boldsymbol{f}(\boldsymbol{x}, \mu) \tag{13}$$

be a system of differential equations where $f(0, \mu) = 0$ for all $\mu$ in a neighborhood of 0. The Jacobian $D_x f(0,0)$ of $f$ in (0, 0) has the eigenvalues $\lambda_{1,2} = \pm j\omega$ with $\omega \neq 0$ and n − 2 other eigenvalues $\lambda_k$ with $\Re\, \lambda_k < 0$. Furthermore $d\ \mathrm{d}\mu\ \Re\ \{\lambda_1\ (\mu)\}|_{\mu=0} > 0$, and the equilibrium point 0 is a stable spiral in $\mu = 0$. Under these assumptions sufficiently small positive numbers $\mu_1$ and $\mu_2$ exist such that for all $\mu \in (-\mu_1, 0)$ the equilibrium point *0* is a stable spiral and for all $\mu \in (0, \mu_2)$ the equilibrium point *0* is an unstable spiral. In the last case the unstable spiral is surrounded by a stable limit cycle whose amplitude increases with $\mu$.

Instead of a proof [see e.g. Hassard et al. (16) or Mathis (5)], this theorem is illustrated by the van der Pol equation.

Example. The van der Pol equation (3) can be formulated by a standard transformation $y := \dot{x}$ into a system of differential equations of first order. Using the normalization $u := \sqrt{\varepsilon}x$ and $v := \sqrt{\varepsilon}y$, the following differential equations result:

$$\dot{u} = v \tag{14}$$

$$\dot{v} = -u - (u^2 - \varepsilon)v \tag{15}$$

The eigenvalues of the Jacobian matrix are

$$\lambda_{1,2} = \frac{\varepsilon}{2} \pm \sqrt{\left(\frac{\varepsilon}{2}\right)^2 - 1} \tag{16}$$

and therefore $\lambda_{1,2} = \pm j$ (for $\varepsilon = 0$) and $d\ d\varepsilon\ \Re\ \lambda_1\ (\varepsilon) \mid_{\varepsilon=0} = \frac{1}{2} > 0$. It can be shown that if $\varepsilon = 0$, the equilibrium point $(u, v) = (0, 0)$ is a stable spiral. It results from the Poincaré–Andronov–Hopf theorem that a stable limit cycle is generated for $\varepsilon > 0$ that encloses an unstable spiral.

This oscillator model and the theorem were formulated for the first time by Andronov and his coworkers in 1934, studying electronic oscillator circuits, but it was 1979 before Mees and Chua published theoretical considerations about oscillator design using this theorem [see Mees (17)]. On the other hand, a necessary condition of this theorem—Barkhausen's oscillatory condition—was a known long time ago and became the basis of a linear design theory for oscillators.

## Design Aspects

**The Linear Design Theory of Sinusoidal Oscillators.** It is known from the Poincaré–Andronov–Hopf theorem that one pair of eigenvalues has to cross the imaginary axis, whereas the other eigenvalues have to remain within the left half complex plane. Obviously, it is a necessary condition that oscillator circuits have a pair of eigenvalues on the imaginary axis for a certain value of some circuit parameter. It is mentioned in the subsection "Oscillator Models" above that this condition can be interpreted as the compensation step of oscillator design, which can be performed in a linear manner using a linear negative resistor. This necessary assumption of the Poincaré–Andronov–Hopf theorem has been known since the first oscillator paper of Vallauri (1) in 1917, and during the following few years several variants of his results were published. One of the most popular criteria was the Barkhausen oscillatory condition [see e.g. Millman and Grabel (9)]. All these variants can be classified by using the following topological structures of oscillator circuits:

- the negative-impedance–admittance model
- the positive-feedback model

and applying corresponding methods of network analysis. It has been known for a long time that these two models are equivalent from a network-theoretical point of view.

Many oscillator circuits contain tubes or transistors. In the case of tuned-circuit oscillators it is more efficient to describe such a circuit as an active 3-pole with a passive impedance embedding (see Fig. 4). This was done for the first time in 1920 by Hazeltine (18). He showed that in Fig 4 the impedances $Z_1$, $Z_2$, and $Z_3$ have to be capacitive, capacitive and inductive, respectively. The reader will find systematic conderations about this subject in the books of Spence (19) and Cassignol (20). Since this rather restricted model for oscillator circuits can be reformulated in the form of the negative-impedance–admittance model or the positive-feedback model, we discuss the use of the latter models in more detail. For this purpose we consider a rather simple oscillator circuit in order to avoid tedious calculations; further examples can be found in textbooks of electronics [e.g. Millman and Grabel (9)].

As the first step the network elements of an actual oscillator circuit have to be associated with the defining blocks of the above-mentioned models. In general this step includes some arbitrariness. The second step uses the conditions that a pair of eigenvalues with vanishing real parts have to occur, formulated for the special topology of the models. As a result we obtain (necessary) conditions for the occurrence of oscillations with respect to the oscillator frequency and the gain of the active elements parametrized by means of the network parameters of an actual oscillator circuit. These conditions represent the linear part of the design of oscillator circuits.

Now we compile the corresponding conditions for the above-mentioned oscillator models (see Parzen (6), Chap. 1):

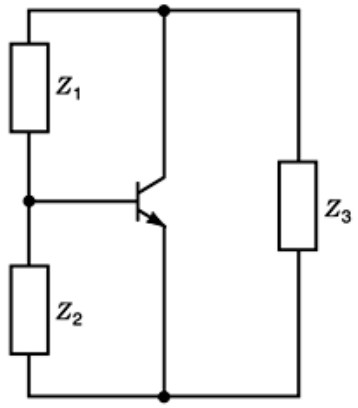


**Fig. 4.** Active 3-pole structure of transistor oscillators.

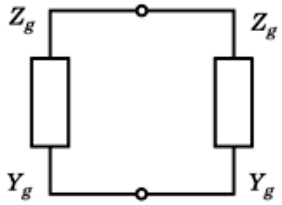


**Fig. 5.** Negative-impedance and admittance oscillator model.

- Negative-impedance model The real and imaginary parts $R$ and $X$, respectively, of the model in Fig. 5 have to satisfy the conditions

$$R_g = -R_L, \quad X_g = -X_L \tag{17}$$

- Negative-admittance model The real and the imaginary parts $G$ and $B$, respectively, of the model in Fig. 5 have to satisfy the conditions

$$G_g = -G_L, \quad B_g = -B_L \tag{18}$$

- Positive-Feedback model The open-loop gain consisting of the transfer functions $A(s)$ and $\beta(s)$, respectively, of the active block and the passive block (see Fig. 6) has to satisfy the condition

$$A\beta = 1 \quad \Leftrightarrow \quad \Re A\beta = 1, \quad \Im A\beta = 0 \tag{19}$$

In the literature these conditions are called the Barkhausen criterion [see e.g. Millman and Grabel (9)]. Instead of the decomposition of the complex equation into the real and the imaginary part, a representation with magnitude and phase angle is preferred.

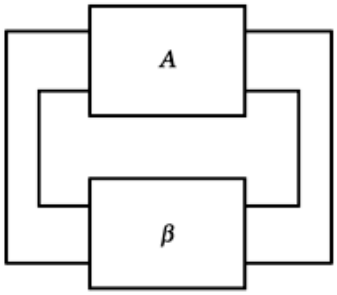


**Fig. 6.** Feedback oscillator model.

Of course, a network analysis in a straightforward manner leads to equivalent conditions for the occurrence of oscillations. For this purpose we consider the ac network model of an oscillator circuit that contains no independent sources and derive its network equations in the frequency domain. As a result we obtain a homogeneous system of linear equations

$$\mathrm{M}(j\omega)x = 0 \tag{20}$$

with the oscillation frequency $j\omega$ as the parameter. Note that an oscillator circuit contains only constant independent sources. Therefore these sources are omitted in the small-signal model. The matrix coefficients contain the network parameters. It is known from linear algebra that nontrivial solutions are obtained if the condition

$$\det\ \mathrm{M}(j\omega) = 0 \tag{21}$$

is satisfied. The equivalence of this expression to the other criteria can be shown.

There is another method that is equivalent to a circuit analysis under certain conditions. In this case a transfer function is defined with respect to a (sinusoidal) input source and two terminal as the output port. This approach can be applied in a successful manner only if

- The input current or voltage source does not change the oscillator circuit substantially, that is, we recover the initial circuit if the input source vanishes
- The circuit is controllable and observable with respect to the chosen input and output ports

The first condition is satisfied if we use pliers entry and an independent voltage source or soldering-iron entry and an independent current source [see e.g. Desoer and Kuh (21)]. For the second condition a careful analysis of the circuit is needed before the two-ports are chosen.

Example: Tunnel Diode Oscillator [Mees (17)]. The nonlinear network equations of the circuit in Fig. 7 can be formulated as (if $R \approx 0$)

$$\frac{d}{dt}\begin{pmatrix} i_L \\ \tilde{u}_C \end{pmatrix} = \begin{pmatrix} 0 & 1/L \\ -1/C & 0 \end{pmatrix}\begin{pmatrix} i_L \\ \tilde{u}_C \end{pmatrix} + \begin{pmatrix} 0 \\ (1/C)g(U_0 - \tilde{u}_C) \end{pmatrix} \tag{22}$$

where $\tilde{u}_C := U_0 - u_C$. Since the constant solution can be calculated in a simple manner as

$$i_L^0 = g(U_0), \qquad \tilde{u}_C^0 = 0 \quad (u_C = U_0) \tag{23}$$

the ac network model (linearized network equations) can be derived without distinction between large and small signal currents and voltages. Let $g'$ be the derivative of $g$ with respect to its argument; then the transformation of this equation into the frequency domain leads to the following condition:

$$\det \begin{pmatrix} 0 & 1/L \\ -1/C & -(1/C)g'(U_0) \end{pmatrix} = \lambda^2 + \frac{1}{C} g'(U_0)\lambda + \frac{1}{LC} = 0 \tag{24}$$

The roots of this quadratic equation are

$$\lambda_{1,2} = -\frac{1}{2C} g'(U_0) \pm \sqrt{\left(\frac{1}{2C} g'(U_0)\right)^2 - \frac{1}{LC}} \tag{25}$$

and therefore a purely imaginary pair of eigenvalues is obtained if the condition

$$\frac{1}{C} g'(U_0) = 0 \tag{26}$$

is satisfied. In this case the oscillator frequency is given by $\omega^2{}_0 = 1/(LC)$. We find from the tunnel-diode characteristic that this is possible if the operating point of the diode is located at its maximum or minimum, where the derivative $g'(U_0)$ vanishes. If the ac network model of this tunnel-diode circuit is interpreted as the negative-conductance model, we find the oscillatory conditions

$$g'(U_0) = 0, \qquad \omega_0 C - \frac{1}{\omega_0 L} = 0 \tag{27}$$

Obviously these conditions are equivalent to the previous one. A negative-resistance model is not suitable in this example. If the negative-conductance model is assumed, a transfer function is determined if an extra (index E) independent sinusoidal voltage source $U_\mathrm{E}$ is located as an input quantity in series with the linearized tunnel diode resistor and the capacitor voltage $U_\mathrm{C}$ is used as output quantity; both $U_\mathrm{E}$ and $U_\mathrm{C}$ are represented in the frequency domain. The corresponding transfer function can be derived:

$$H(j\omega) = \frac{U_C}{U_\mathrm{E}} = \frac{g'(U_0) j\omega L}{1 - \omega^2 LC + j\omega g'(U_0) L} \tag{28}$$

The zeros of the denomiator are the eigenvalues of this circuit. Under the same condition $[g'(U_0) = 0]$ on the voltage $U_0$, we obtain a pair of imaginary eigenvalues and the oscillatory frequency) given by $\omega^2 = 1/LC$. Finally we consider the approach where the positive-feedback model is applied. For this purpose we reformulate the negative-conductance model so that the conductances $Y_\mathrm{g} = g'(U_0$ and $-Y_L(j\omega) = -1/Z_L(j\omega)$ become identical, that is the sum of the admittances $Y_g$ and $Y_L$ has to be zero. By means of $Z_L(j\omega)$ an interpretation as a product

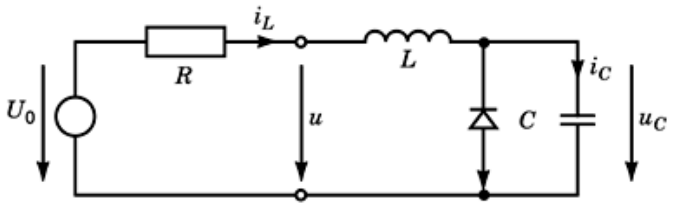


**Fig. 7.** Tunnel-diode oscillator model.

is possible if the sum is reformulated as

$$Y_g Z_L(j\omega) = g'(U_0)\frac{-1}{j\left(\omega_0 C - 1/\omega_0 L\right)} = 1 \qquad (29)$$

This is Barkhausen's condition if $Y_g$ and $-Z_L(j\omega)$ are interpreted as transfer functions of a feedback model. Since this reformulation is derived by means of equivalent calculation steps, the same conditions for the occurrence of oscillations are obtained. Probably it is rather a problem of taste and/or experience which approach is used to derive the oscillatory conditions. For example, Parzen (6) discusses the design of tuned-circuit oscillators with transistors, and therefore he uses the above mentioned active three-pole representation with passive embedding. Based on this model, the author applies the negative-resistance–conductance model to calculate the oscillatory conditions. Mauro (27), prefers the positive-feedback model and derives similar conditions for tuned-circuit oscillators as well as *RC* oscillators. In general both approaches can be used successfully, and therefore the choice makes no difference from a theoretical point of view.

**The Nonlinear Design Aspects of Sinusoidal Oscillators.** Although many aspects of the nonlinear theory of oscillator circuits are known, it is not trivial to make use of them to construct a systematic design concept for these circuits. The theoretical results are at least suitable for a classification of oscillator circuits and for the construction of simulation tools. We will discuss these subjects in this and the following sections. Just as in other cases of circuit design, an oscillator circuit is determined if its network topology as well as its network parameters is known. A design process starts with some specifications of the desired oscillator circuit, and then we try to find an oscillator topology together with a certain set of network parameters in order to fit these specifications. For this purpose the following approach can be used. Further details can be found for example, in the monograph of Parzen (6).

(1) *Basic Specifications* The form of the oscillator behavior (sinusoidal, rectangle, triangle, etc.), frequency of the oscillator, the amplitude, and so on, are taken into consideration.
(2) *Choice of the Circuit Devices* The application of the oscillator circuit, the working temperature, and so on, are taken into consideration.
(3) *Choice of the Type of Resonator* The frequency stability, the amplitude stability, the variability of the frequency, and the economic expense are taken into consideration.
(4) *Choice of the Kind of Limiting that Maintains the Oscillator Amplitude* A self-limiter, external limiting, or automatic-level-control limiting can be chosen.
(5) *First Draft of the Oscillator Circuit* The above aspects are taken into consideration.
(6) *Determination of Circuit Parameters* The actual circuit devices and its circuit parameters have to be chosen.
(7) *Optimization* Circuit simulations and/or an experimental realization are necessary. If the circuit does not meet the specifications, then some steps have to be repeated.

## 12 OSCILLATOR DESIGN

This design summary shows that each design process of an oscillator circuit presents peculiar problems. However, we will make some general remarks based on the theoretical considerations above. Although the frequency of an sinusoidal oscillator can be determined by a linear analysis (see the Barkhausen condition in the previous subsections, in view of the Poincaré–Andronov–Hopf theorem nonlinearities are essential for the functionality of oscillators (see the subsection "Oscillator Models" above). We already mentioned in that subsection that a nonlinearity is necessary for limiting the amplitude. This can be provided in one of three ways:

(1) *Self-Limiting* The inherent linearity of an active device (tube, transistor, operational amplifier, etc.) is used to build up a nonlinear differential equation with a stable limit cycle. In this case the amplitude is fixed implicitly by the type of nonlinear characteristic. The only requirement is to calculate the amplitude with a suitable model of the nonlinear device.

(2) *External Limiting* This is a variant of the first case, since the resonant circuit works in a linear mode and the limiting is introduced by an additional device (Zener diode, symmetrical clippers, thermistors, etc.).

(3) *Automatic-Level-Control Limiting* The natural approach to limiting is amplitude control—that is, measuring the amplitude, comparing it with a desired amplitude value, and adjusting (if necessary) a circuit parameter that controls the damping of the circuit through a suitable control strategy. Even if the resonant circuit is approximately linear, the entire circuit, including the control part, is nonlinear because there is a coupling between at least one state variable and a circuit parameter. A suitable discussion for the construction of such control devices can be found in the monograph of Parzen (6) and the dissertation of Meyer-Ebrecht (23).

The first way of limiting of the oscillator amplitude leads to a rather simple construction of the oscillator circuit, but in this way the damping element is influenced by the large signal gain factor. Unfortunately, this gain factor varies with the instantaneous amplitude of the oscillator and results in spectral distortions. This is an essential disadvantage in the case of sinusoidal oscillators. If such an oscillator with low distortion is desired, the nonlinear damping should depend on an indefinite integral $\int x(t)\,dt$ of the amplitude $x(t)$ instead of the instantaneous amplitude. In mathematical terms this statement can be formulated as follows if we restrict our discussion to an oscillator circuit of van der Pol type. Then the descriptive equation is of the form

$$\ddot{x} + \gamma\left(\int x(t)\,dt\right)\dot{x} + \omega^2 x = 0 \tag{30}$$

instead of

$$\ddot{x} + \gamma(x)\dot{x} + \omega^2 x = 0 \tag{31}$$

Although the structure of an oscillator circuit and its amplitude stabilization are essential, analysis methods are necessary in order to calculate at least the amplitude and the frequency as a function of certain circuit parameters for a suitable design of a sinusoidal oscillator. Since analytical solutions of the corresponding network equations of an oscillator are not available, perturbation methods have to be applied for this purpose. Several approaches are available:

- Perturbation methods
- Averaging or harmonic balance, methods

- Describing-function method
- Volterra series method

Most of the different variants of perturbation methods start with some Fourier polynomial and, based on this first step derive a set of associated differential equations. Therefore these methods can be interpreted as time-domain methods, which are considered and illustrated in the monograph of Nayfeh (24). The first-order perturbation results are of special interest in practical oscillator design. Also the averaging (harmonic balance) methods can be interpreted as time-domain methods. A very efficient variant of an averaging method that can be implemented in a computer algebra program uses Lie series [see Kirchgraber and Stiefel (25)]. It was applied for studying electronic oscillators by Keidies and Mathis (26).

Another time-domain method can be interpreted as an extension of the convolution description of linear time-invariant input–output systems, which is implemented in Volterra series methods. In this case a series of integrals is used as a first step and the coefficients are convolution kernels of higher order. Illustrations of this method are included in the paper of Chua and Tang (27).

An efficient iterative procedure for calculating the steady-state output waveform of almost sinusoidal nonlinear oscillators using the feedback formulation is presented by Buonomo and Di Bello (28). In their paper this method is compared with the alternative methods of Mathis and Keidies as well as Chua and Tang. Just like the other methods, the interative approach can be implemented by means of a computer algebra system.

Since frequency-domain methods are very successful in the case of linear time-invariant circuits and systems, many electrical engineers are greatly interested in extensions of these approaches to nonlinear circuits and systems. The describing-function method is very popular because it can be interpreted as an extension of the transfer-function method, which is a standard method in the analysis of linear time-invariant networks. We have to assume that only the first-harmonic part of the response of a nonlinear block to a sinusoidal input function is of interest, because the other parts will be filtered out. If the functionality of the sinusoidal oscillator is interpreted in terms of the feedback structure in Fig. 6, this filter is realized within the feedback loop. Although the nonlinear block produces an entire spectrum of output frequencies as a response to a sinusoidal input function, only the first-harmonic part is essential for the functionality of a sinusoidal oscillator. Therefore the describing-function method is illustrated by means of the feedback model of a sinusoidal oscillator, although extensions of the negative-impedance and admittance models, respectively, are possible [see e.g. Cassignol (20)].

We restrict our discussion to the case where only the $A$ block in Fig. 6 contains nonlinear elements and the input signal is $x(t) = \bigcirc \cos \omega t$. Then a first-harmonic part can be extracted from the output signal

$$y(t) = y_1 \cos(\omega t + \varphi_1) + y_2 \cos(2\omega t + \varphi_2) + \cdots \tag{32}$$

where we assume that no constant part is included in the output signal. Clearly the amplitudes $y_1, y_2$, and the phases $\varphi_1, \varphi_2, \ldots$ depend on $\bigcirc$ and $\omega$. The describing function is defined by

$$N(\hat{x}, \omega) = \frac{y_1(\hat{x}, \omega)}{\hat{x}} e^{j\varphi_1(\hat{x}, \omega)} \tag{33}$$

As a result we obtain a generalization of the Barkhausen oscillatory condition:

$$N(\hat{x}, \omega)\beta(\omega) = 1 \tag{34}$$

In many cases $N(\bigcirc \omega)$ is independent of $\omega$. Then $\beta(\omega)$ can be plotted as a single polar curve in the complex plane, graduated in $\omega$, and likewise the locus of $-1/N(\bigcirc)$ can be plotted, graduated in $\bigcirc$. The intersection

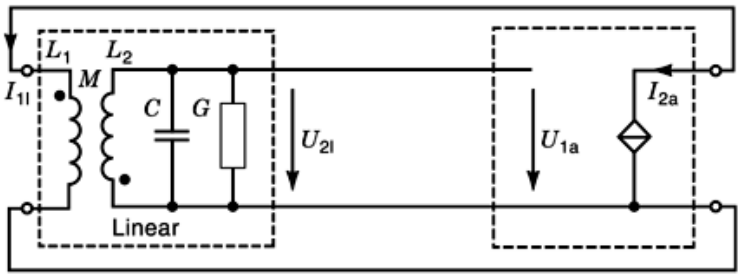


**Fig. 8.** Two-port oscillator.

of these curves corresponds to a limit cycle, whose stability properties can be studied. More details of this approach are included in the monograph of Mees (17), where its problems are also discussed.

**Design of Two-Port Oscillators.** In the following we consider the two-port oscillator formed by a frequency-dependent linear feedback two-port and a nonlinear active two-port as depicted in Fig. 8. The output signal of the linear two-port is amplified in the nonlinear active two-port and then fed back to the input of the linear two-port. A necessary condition for the occurrence of a stationary harmonic oscillation is that the phase and the amplitude of the signal, after passing both two-ports, are unchanged. Due to the frequency-dependent linear feedback two-port, the phase condition is only fulfilled for one frequency. Due to the nonlinearity of the active two-port, the amplitude condition is only fulfilled for one value of the amplitude of the signal.

In our example we consider the simple model of an active two-port formed by a voltage-controlled current source. The voltage–current characteristic of the voltage-controlled current source is assumed to be nonlinear. If the active two-port contains additional linear elements, these elements may be moved to the linear two-port. In our example the linear frequency-dependent two-port consists of a transformer with primary inductance $L_1$, secondary inductance $L_2$, and mutual inductance $M$; a capacitor $C$; and a conductor $G$. The primary and secondary coils of the transformer are in antiphase, and therefore $M < 0$. The secondary inductance $L_2$ and the capacitor $C$ together form a parallel resonant circuit. This inductor-coupled resonant circuit is the most compact model we can establish for the linear feedback circuit.

In more complex cases we can replace the reactive part of the feedback two-port by the canonical Foster representation (29). In the neighborhood of the resonant frequency the essential part of the canonical Foster realization is given by a transformer-coupled resonant circuit, as assumed in our model. In the case of small losses it is also possible to include the losses in this model (30). The conductor $G$ accounts for the losses in the passive and the active two-ports. At the resonant frequency of the parallel resonant circuit,

$$\omega_0 = 1/\sqrt{L_2 C} \tag{35}$$

the phase change in the linear two-port is 180°. This compensates for the 180° phase change occurring in the active circuit, and the phase condition for oscillation is fulfilled.

The nonlinear dependence of the output current $i_{2a}(t)$ of the linear two-port on its input voltage $i_{1a}(t)$ is given by

$$i_{2a}(t) = f\big(u_{1a}(t)\big) \tag{36}$$

The active two-port is considered to be frequency-independent. It is assumed that all reactive elements of the active element have been moved to the linear two-port. This can be done easily if the reactive elements are linear, and if it is possible to concentrate all reactive elements in a Π equivalent circuit. The relation between

the spectra of the input current $I_{1l}(\omega)$ and the output voltage $U_{2l}(\omega)$ of the linear feedback network is given by

$$I_{1l}(\omega) = A_{21}(\omega)U_{2l}(\omega) \tag{37}$$

where $A_{21}$ is the matrix element of the chain two-port representation. According to Fig. 8 we obtain $u_{1a} = u_{2l}$ and $i_{1l} = -\,i_{2a}$. Furthermore, we consider $i_{1l}(t)\ I_{1l}(\omega)$ and $u_{2l}(t)\ U_{2l}(\omega)$, where $(\cdot)(t)\ (\cdot)(\omega)$ denotes in a symbolic manner a pair of Fourier-transformed functions in time and frequency domain.

We assume that in the oscillator circuit, Fig. 8, oscillations are excited by an initial perturbation. After some period of growth of amplitude due to the nonlinearity of the active element, the oscillator will saturate in a stationary state oscillating at a frequency $\omega_0$. In the case of a weak nonlinearity the oscillation exhibits only low harmonics. The linear feedback network acts as a bandpass filter and attenuates the harmonics. In the case of a sufficiently high $Q$ factor of the resonant circuit and a weakly nonlinear active element, the transient of the oscillator from excitation to the stationary state exceeds the period of oscillation by orders of magnitude. We also can assume that the time constants governing the decay of the perturbation of the stationary state of the oscillator exceed the period of oscillation by orders of magnitude. Under these assumptions we can make for $u_{2l}$ the first step

$$u_{2l}(t) = V(t)\ \cos[\omega_0 t + \varphi(t)] \tag{38}$$

where $V(t)$ and $\varphi(t)$ denote the amplitude and the phase of the oscillator signal. Due to the nonlinearity of the active two-port, the output amplitude $I$ at the fundamental frequency $\omega_0$ depends nonlinearly on the input amplitude $V$. With $\omega_0 t = \xi$ we obtain from Eq. (36) the fundamental frequency component of the output current,

$$I(V) = \frac{1}{\pi}\int_0^{2\pi} f(V\ \cos\ \xi)\ \cos\ \xi\, d\xi \tag{39}$$

This relation holds also for slowly time-varying amplitudes, and we obtain

$$i_{2a} = I\big(V(t)\big)\ \cos[\omega_0 t + \varphi(t)] \tag{40}$$

With $a_{21}(t)\ A_{21}\ (\omega)$ we obtain from Eq. (37) the relation between the input current $i_{1l}(t$ and the output voltage $u_{2l}(t$ of the linear feedback circuit in the time domain:

$$i_{1l}(t) = \int_{-\infty}^{+\infty} a_{21}(t - t_1)u_{21}(t_1)\, dt_1 \tag{41}$$

Representing Eq. (40) by

$$u_{2l}(t) = \Re\left(V(t)\ \exp\{j[\omega_0 t + \varphi(t)]\}\right) \tag{42}$$

and expanding into a first-order power series yields

$$u_{2l}(t_1) = \Re\left[\left(V(t) + (t_1 - t)\{\dot{V}(t) + j[\omega_0 t + \dot{\varphi}(t)]V(t)\}\right)\exp\{j[\omega_0 t + \varphi(t)]\}\right] \tag{43}$$

Inserting this expression into Eq. (41) gives

$$i_{1l}(t) = \Re\left( V(t)e^{j[\varphi(t)+\omega_0 t]} \int_{-\infty}^{+\infty} a_{21}(t-t_1)e^{j\omega_0 t_1}\, dt_1 \right. \tag{44}$$

$$\left. -[\dot{V}(t) + j\dot{\varphi}V(t)]e^{j[\varphi(t)+\omega_0 t]} \int_{-\infty}^{+\infty} (t-t_1)a_{21}(t-t_1)e^{j\omega_0 t_1}\, dt_1 \right) \tag{45}$$

With the substitution $t - t_1 = t_2$ we obtain

$$i_{1l}(t) = \Re\left[ \left( V(t)e^{j[\varphi(t)+\omega_0 t]} \int_{-\infty}^{+\infty} a_{21}(t_2)e^{j\omega_0 t_2} dt_2 \right. \right. \tag{46}$$

$$\left. \left. -[\dot{V}(t) + j\dot{\varphi}V(t)]e^{j[\varphi(t)+\omega_0 t]} \int_{-\infty}^{+\infty} t_2 a_{21}(t_2)e^{-j\omega_0 t_2}\, dt_2 \right) e^{j[\varphi(t)+\omega_0 t]} \right] \tag{47}$$

Using $a_{21}(t)\, A_{21}(\omega)$ and $t a_{21}(t)\, j A'_{21}(\omega)$ with $A'_{21}(\omega) = dA_{21}(\omega)/d\omega$, we obtain

$$i_{1l}(t) = \Re\left( \left\{ V(t)A_{21}(\omega_0) + [\dot{\varphi}V(t) - j\dot{V}(t)]A'_{21}(\omega_0) \right\} e^{j[\omega_0 t+\varphi(t)]} \right) \tag{48}$$

With Eq. (40) and $i_{1l} = -i_{2a}$ it follows that

$$\Re\left( \left\{ I\big(V(t)\big) + V(t)A_{21}(\omega_0) + \big[\dot{\varphi}V(t) - j\dot{V}(t)\big]A'_{21}(\omega_0) \right\} e^{j[\omega_0 t+\varphi(t)]} \right) = 0 \tag{49}$$

Introducing the conductance $G_0$ and the susceptance $B_0$ by

$$G_0(\omega_0) = -\Re A_{21}(\omega_0), \qquad B_0(\omega_0) = -\Im A_{21}(\omega_0) \tag{50}$$

yields

$$I(V) - VG_0 - \dot{\varphi}VG'_0 - \dot{V}B'_0 = 0 \tag{51}$$

$$VB_0 + \dot{\varphi}VB'_0 - \dot{V}G'_0 = 0 \tag{52}$$

where the prime $(\cdot)'$ denotes the derivative with respect to $\omega$ evaluated at $\omega = \omega_0$. For the stationary state it follows that

$$I(V_0) - V_0 G_0(\omega_0) = 0 \tag{53}$$

$$B_0(\omega_0) = 0 \tag{54}$$

We now investigate the influence of small perturbations $V_1$ of the stationary amplitude $V_0$. With the first step

$$V = V_0 + V_1 \tag{55}$$

we linearize $I(V) - VG_0$ in a neighborhood of the stationary amplitude $V_0$. With

$$I(V) - VG_0 \approx I(V_0) + V_1 I'(V_0) - V_0 G_0 - V_1 G_0 = V_1(I'(V_0) + G_0) \tag{56}$$

we obtain for small-amplitude deviations $V_1$ from the stationary state the linear differential equation

$$\dot{V}_1 + \frac{B_0'(G_0 - I')}{B_0'^2 + G_0'^2} V_1 = 0 \tag{57}$$

The stationary state of oscillation is stable if any perturbation $V_1$ is decaying. This holds for

$$\frac{dB_0}{d\omega}\left(G_0 - \frac{dI}{dV}\right) > 0 \tag{58}$$

The relation between $I$ and $V$ may be expressed by a nonlinear transconductance $S$ given by

$$S(V) = \frac{I}{V} \tag{59}$$

In this case the stability condition (58) can be written in the following form:

$$\frac{dB_0}{d\omega}\frac{dS}{dV} < \frac{dB_0}{d\omega} G \tag{60}$$

For the Meissner oscillator with transformer feedback circuit according to Fig. 8 the parameters $G_0$ and $B_0$ are given by

$$G_0 = \frac{L_2}{|M|} G \tag{61}$$

$$B_0 = \frac{L_2}{|M|}\left(\omega C - \frac{1}{\omega L_2}\right) \tag{62}$$

The condition (54) yields the frequency of oscillation $\omega_0$ in the stationary state according to Eq. (35). Due to Eq. (53), the stationary amplitude $V_0$ can be determined from

$$S(V_0) = \frac{L_2}{|M|} G \tag{63}$$

From

$$\left.\frac{dB_0(\omega)}{d\omega}\right|_{\omega=\omega_0} = 2\frac{L_2 C}{|M|} \tag{64}$$

and Eq. (60) it follows that the stationary state of the two-port oscillator considered is stable for

$$\frac{dS}{dV} < 0 \tag{65}$$

that is, for a transconductance $S$ that decreases with increasing amplitude $V$.

**Design of Relaxation Oscillators.** In the subsection "Oscillator Models" it was mentioned that the van der Pol equation is suitable also as a model for relaxation oscillators if $\varepsilon << 1$ is considered. Unfortunately, analytical solutions are not available in this case, and for the derivation of approximative solutions advanced mathematical methods are necessary [see e.g. Andronov et al. (2) or Mathis (5)]. Therefore almost all design methods for relaxation oscillators are based on more simplified models for the active devices (e.g. transistors or operational amplifiers). If the transistors are replaced by switches [see e.g. Horenstein (31)] we obtain piecewise linear oscillator models; note that such models are nonlinear, as was always the case. Some disadvantages of this approach are known:

- The transient to the steady state (or limit cycle) cannot be obtained in a simple manner.
- A limit cycle has to be assumed.
- The results are independent of certain parameters of the active devices.

However, under these assumptions simple design formulas can be derived, since only linear (time-invariant) networks have to be analyzed. We illustrate this approach in the case of a symmetrical multivibrator that is working in saturated mode. More complicated situations (e.g. if transistors are not working in saturated mode) will be found for example in Gray and Meyer (32).

Example: Symmetrical Multivibrator. We consider the multivibrator that is shown in Fig. 9. Let us assume that at the initial instant $t = 0$, the left transistor $T_1$ conducts and the right transistor $T_2$ is cut off. If the voltage across the left capacitor is near to zero while that across the right capacitor reaches the voltage $U_0$, a switching event occurs. During the commutation where $T_1$ switches to the cut-off state while $T_2$ changes to the conducting state, the left Capacitor charges and the right capacitor discharges. The situation for $t > 0$ can be analyzed by means of a simple analysis of the network in Fig. 10. The following differential equation results:

$$R_b C\frac{du_C}{dt} + u_C = U_0 \tag{66}$$

where $u_C(0) = U_0$. The solution is derived by well-known calculations:

$$u_C(t) = -U_0\left(1 - 2e^{-t/R_b C}\right) \tag{67}$$

A switching event takes place if $u_C(t)$ that corresponds to the base–emitter voltage of $T_2$ exeeds the cutoff voltage (which is simplified to zero in our case). From the above solution we have

$$t_{sw} := R_b C \ln 2 \approx 0.69\, R_b C \tag{68}$$

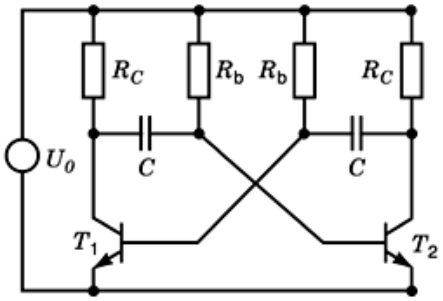


**Fig. 9.** Symmetrical multivibrator.

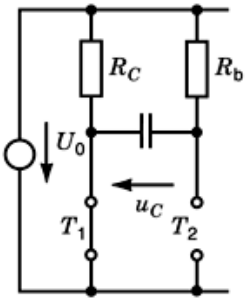


**Fig. 10.** Dynamic operation.

and therefore the period of the square wave is $T \approx 1.38\,R_bC$. It is an easy matter to include cutoff and saturation quantities for the transistors [e.g. Cassignol (20)]. In the same way, results for other relaxation oscillators can be derived that include operational amplifiers or digital gates [see e.g. Horenstein (31) or Kurz and Mathis (33)]. Furthermore, saw tooth-wave oscillators can be analyzed if piecewise linear models of the active devices are used. The reader is referred to the literature for further details [e.g. Davidse (34)].

## Advanced Microwave Oscillator Design Tools

**Problems in Microwave Oscillator Design.** Although this article is concerned with design methods for all kinds of oscillators, the design of microwave oscillators has been of special interest during the last 15 years. Many results are published in the literature. Therefore an overview is presented in this section. But it should be mentioned that almost all methods can be used to design other kinds of oscillators.

The design of monolithic integrated microwave and millimeter-wave oscillators requires accurate and efficient tools for numerical modelling and optimization. Today the design of microwave oscillators in many cases is based on a linear analysis of the oscillation conditions. To predict and to optimize the oscillator output power or the oscillator spectral behavior, however, a nonlinear design approach is indispensable.

The task of oscillator modeling can be separated into two parts:

- Nonlinear modeling of the unperturbed oscillator
- Modeling of the noise properties of the oscillator

The nonlinear modeling of the unperturbed oscillator may be done in the time domain by numerical integration (35,36,37) in the frequency domain using harmonic balance or Volterra series methods (38,39, 40,41,42) or by using combined time–frequency-domain methods (43,44,45,46). Microwave oscillators may be subdivided into a linear embedding circuit and one or more nonlinear subcircuits. By this subdivision, the computational effort may be reduced considerably. The easiest approach is to subdivide the active element of the oscillator into a linear embedding network and a single nonlinear controlled source. In this way, the modeling may be improved over the linear approach, as shown for example in Refs. 47,48. This method is restricted to a single dominant nonlinearity in the oscillator circuit.

More accurate circuit modeling requires the inclusion of numerous nonlinear circuit elements in the simulation. Approximating the distributed elements within a broad but finite frequency interval by a lumped-element equivalent circuit facilitates the description of the unperturbed network by a set of nonlinear and autonomous first-order differential equations in the normal form

$$\frac{dx}{dt} = f(x), \quad x \in IR^N \tag{69}$$

The components of the vector $x$ are the state variables of the system. Time-domain integration of the network equations describing the equivalent lumped-element circuits usually requires an enormous computational effort, since the system of differential equations is usually high-dimensional and also exhibits high stiffness. One method for reducing the computational effort is to combine time-domain and frequency-domain calculations (43). The periodic steady-state solution can be found in the time domain by solving the periodic boundary-value problem (35). The solution obtained in the time domain is exact and in this respect superior to that from harmonic balance. Using the multiple shooting algorithm of Bulirsch, the convergence of the time-domain boundary-value problem may be improved (49,50).

Schwab et al. have applied the time-domain boundary-value method to the self-consistent determination of the steady-state solution of oscillators (37). The time-domain method has the advantage that it is not necessarily restricted to a certain number of harmonics of the signals.

The most common method for frequency-domain analysis of oscillators is the harmonic balance method. Using that method, a nonlinear system of equations

$$F(X, \omega_0) = 0, \quad X \in \mathbb{C}^{n(2k+1)} \tag{70}$$

has to be solved. In this equation $X$ is the system state vector summarizing the amplitudes of $n$ signals at the fundamental frequency $\omega_0$ and at $K$ harmonics (38,39,40,41,42). The advantage of the harmonic balance method is that distributed circuits can also be considered in the analysis.

In the combined time–frequency-domain method the oscillator circuit is subdivided into a linear circuit and a nonlinear circuit (43,44). The linear part of the circuit is described in the frequency domain, whereas a state-variable description in time domain is applied to the nonlinear part. This allows one to combine the advantages of frequency-domain and time-domain methods. In the linear part of the circuit, distributed circuit elements can also be considered.

**Time-Domain Method.** The computation of the steady-state solution of the oscillator by solving the initial-value problem (86) for $t \to \infty$ has the disadvantage of large numerical effort. For most practical cases interest is restricted to the periodic steady-state solution $x(t) = x(t + T^0)$ for the nonlinear oscillator waveform. The period of oscillation $T^0$ is not known. In order to determine it we include $T^0$ as an additional variable with the state variables $x$ and introduce the normalized time variable $\tau = t/T^0$. We have now to solve the two-point

boundary-value problem for $\tau \in [0,1]$:

$$\frac{d}{d\tau}\boldsymbol{x} = f(\boldsymbol{x})T^0, \quad \frac{dT^0}{d\tau} = 0, \quad \tau = \frac{t}{T^0} \tag{71}$$

The $n + 1$ boundary conditions are

$$\boldsymbol{x}(0) = \boldsymbol{x}(1), \quad x_\kappa = a \tag{72}$$

where the last condition fixes the phase of the limit cycle. Let us denote the solution of the initial-value problem (71) at $\tau_{\mu+1}$ with the initial conditions $s_\mu$ at $\tau_\mu$ by $e(s_\mu, \tau_\mu, \tau_{\mu+1})$. The solution of the boundary-value problem is equivalent to the determination of the zeros of the vector-valued function

$$\boldsymbol{G}(\boldsymbol{x}(0), T^0) = \begin{pmatrix} \boldsymbol{x}(\tau = 0) - \boldsymbol{e}(\boldsymbol{x}(0), \tau_1 = 0, \tau_2 = 1) \\ x_\kappa(0) - a \end{pmatrix} \tag{73}$$

This algorithm is called the single-shooting method, and in general it has only a small domain of convergence.

A better way to solve the boundary-value problem is to use the multiple-shooting algorithm (43,49,50). This algorithm is more stable and has a wider domain of convergence than the single-shooting one. By this method the region between the boundaries is divided into several subregions,

$$0 = \tau_0 < \tau_1 < \cdots < \tau_{\mu-1} < \tau_\mu = 1 \tag{74}$$

and for every subregion a starting point is chosen:

$$\begin{aligned} \boldsymbol{s}_0 &= \boldsymbol{x}(\tau = \tau_0) \\ \boldsymbol{s}_1 &= \boldsymbol{x}(\tau = \tau_1) \\ &\vdots \end{aligned} \tag{75}$$

$$\boldsymbol{s}_{\mu-1} = \boldsymbol{x}(\tau = \tau_{\mu-1}) \tag{76}$$

These starting points are varied until a continuous solution fulfilling the boundary condition is found, which can easily be seen to be the zero of the vector-valued function

$$\boldsymbol{u}(\boldsymbol{s}_0, \boldsymbol{s}_1, \ldots, \boldsymbol{s}_{\mu-1}) = \begin{pmatrix} \boldsymbol{e}(\boldsymbol{s}_0, \tau_0, \tau_1) - \boldsymbol{s}_1) \\ \boldsymbol{e}(\boldsymbol{s}_1, \tau_1, \tau_2) - \boldsymbol{s}_2) \\ \vdots \\ \boldsymbol{e}(\boldsymbol{s}_{\mu-1}, \tau_{\mu-1}, \tau_\mu) - \boldsymbol{s}_0) \\ x_\kappa(0) - a \end{pmatrix} \tag{77}$$

where the last two rows represent the boundary conditions and the others the continuity conditions.

Because of the special structure of Eq. (77), the zeros can be computed in a very efficient way (49). To achieve starting values for $T_0$ and $x$, the set of nonlinear differential equations (86) is linearized at the unstable stationary point $x_0$, with the Jacobian

$$\boldsymbol{J} = \left.\frac{\partial \boldsymbol{F}(\boldsymbol{x})}{\partial \boldsymbol{x}}\right|_{\boldsymbol{x}=\boldsymbol{x}_0} \tag{78}$$

with $x_0$ given by $\boldsymbol{F}(x_0) = 0$. Then $T^0$ and $x(t)$ can be estimated by

$$\boldsymbol{x}(t) = a\boldsymbol{e}_v e^{j\lambda_v t}, \qquad T^0 = \frac{2\pi}{\mathrm{Im}\lambda_v} \tag{79}$$

where $\lambda_1,\ldots,\lambda_n$ the $n$ eigenvalues and $e_1,\ldots,e_n$ the corresponding eigenvectors of the Jacobian $\boldsymbol{J}$. Here $\lambda_v$ is the eigenvalue with $\Re\ \lambda_v > 0$. The stiff-stable Gear algorithm (36) has proven to be an effective method for numerical integration.

**Frequency-Domain Method.** Using the harmonic balance technique, the steady state of the unperturbed oscillator may be computed in the frequency domain. The $n$ state variables of the oscillator are summarized in the state vector $\boldsymbol{X}$:

$$\boldsymbol{X} = (\boldsymbol{X}_1, \boldsymbol{X}_2, \ldots, \boldsymbol{X}_n)^{\mathrm{T}} \tag{80}$$

Since all state variables are periodic in the limit cycle, the time-domain state variables $x_i$ can be expanded into Fourier series with the Fourier coefficients $X_{i,l}$. The frequency range considered is limited to $K$ harmonics:

$$\boldsymbol{X}_i = \left(X_{i,-k}, \quad X_{i,-k+1}, \quad \ldots, \quad X_{i,0}, \quad \ldots, \quad X_{i,+k}\right)^{\mathrm{T}}, \quad \text{with} \quad \boldsymbol{X}_i \in \mathbb{C}^{2k+1} \tag{81}$$

The Fourier coefficients of the state variables $\boldsymbol{X}^0$ are determined by the solution of a nonlinear system of equations

$$\boldsymbol{F}(\boldsymbol{X}^0, \omega_0) \equiv \boldsymbol{0} \tag{82}$$

This system, with dimension $n(2k + 1)$ and $n(2k + 1)$ unknowns, exhibits an infinite one-dimensionl manifold of solutions, since the phase of a free-running oscillator is arbitrary. The solution can be made unique by specifying the phase of one Fourier coefficient. The frequency of oscillation is an unknown variable and is also determined by solution of the system equations.

**Time–Frequency-Domain Method.** Time-domain methods are efficient for the analysis of circuits exhibiting strong nonlinearities. However, it is not possible to include linear distributed circuits in the time-domain analysis. Especially in microwave oscillator design, the linear embedding circuits usually contain distributed circuits. The method described in the following is based on the subdivision of the oscillator network into the following two subsets:

- The linear embedding network
- The nonlinear subnetworks with neighboring low-pass structure

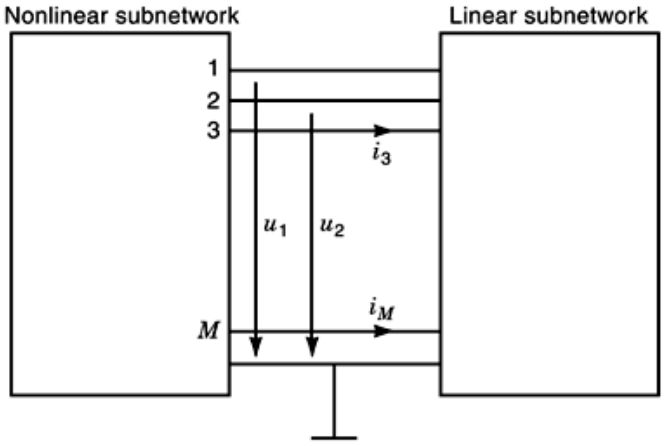


**Fig. 11.** Linear and nonlinear parts of oscillator Network.

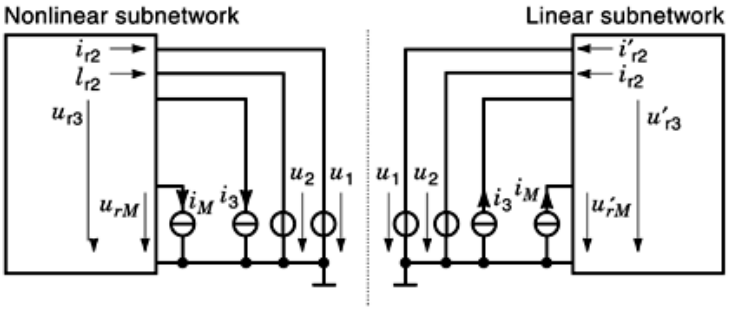


**Fig. 12.** Separation of the linear and nonlinear network parts.

Therefore the network can be represented by a circuit model as shown in Fig. 11.

The linear embedding network may be described effectively in the frequency domain. The linear and nonlinear parts of the oscillator network are connected via a number $M$ of ports. The port voltages and currents are described by the vector $\boldsymbol{l}(t) = [\boldsymbol{v}_T(t), \boldsymbol{i}_T(t)]^T$. Nonlinear resistors and nonlinear conductances are replaced by voltage and current sources and described, in common with all other sources within the nonlinear subnetwork, by the vector $\boldsymbol{l}(t) = [\boldsymbol{v}_0(t), \boldsymbol{i}_0(t)]^T$. In a subsequent step the linear and the nonlinear subnetworks are separated from each other, and the port voltages and currents represented by the vector $\boldsymbol{l}(t)$ are also replaced by voltage and current sources, as shown in Fig. 12.

Based on the time-domain description (36), the nonlinear subnetwork is characterized by

$$\dot{\boldsymbol{x}} = \boldsymbol{A}\boldsymbol{x} + \boldsymbol{B}\boldsymbol{w} + \boldsymbol{C}\dot{\boldsymbol{w}} + \boldsymbol{D}\boldsymbol{l}, \qquad \boldsymbol{x} \in IR^N, \quad \boldsymbol{l} \in IR^M \tag{83}$$

where $\boldsymbol{x}$ are the independent state variables, and $\boldsymbol{w}$ is a function of the state variables and their time derivatives, $\boldsymbol{w} = \boldsymbol{w}(\boldsymbol{w}, \dot{x})$. The matrices $\boldsymbol{A}$, $\boldsymbol{B}$, $\boldsymbol{C}$, and $\boldsymbol{D}$, representing also nonlinear capacitors and inductors, depend on $\boldsymbol{x}$ and $\dot{x}$. Due to the dependence of the matrices $\boldsymbol{A}$, $\boldsymbol{B}$, $\boldsymbol{C}$, $\boldsymbol{D}$ and the vector $\boldsymbol{w}$ on $\dot{x}$, the system of differential equations (83) is implicit. This system can be made explicit and put into the normal form by imposing the condition that the matrices $\boldsymbol{A}$, $\boldsymbol{B}$, $\boldsymbol{D}$ and vector $\boldsymbol{w}$ depend only on $\boldsymbol{x}$ and not on $\dot{x}$. This condition is fulfilled if:

- In the nonlinear subnetwork no current source is connected to a node that is connected only to current sources and to inductors.
- In the nonlinear subnetwork no voltage source is within a mesh containing only voltage sources and capacitors.

Under these conditions the matrix $\boldsymbol{C}$ vanishes. If we also require that $w$ depend only on the system state variables $x$ and not on their time derivatives, we obtain from Eq. (83)

$$\dot{\boldsymbol{x}} = \boldsymbol{A}(\boldsymbol{x})\boldsymbol{x} + \boldsymbol{B}(\boldsymbol{x})\boldsymbol{w}(\boldsymbol{x}) + \boldsymbol{D}(\boldsymbol{x})\boldsymbol{l}(t) \tag{84}$$

The vector $\boldsymbol{c}^T(t) = [\boldsymbol{i}_r\,(t), \boldsymbol{u}_r(t)]$, dual to $\boldsymbol{l}(t)$, is given by

$$\boldsymbol{c}(t) = \boldsymbol{F}\boldsymbol{x} + \boldsymbol{G}\boldsymbol{w} + \boldsymbol{H}\boldsymbol{l} \tag{85}$$

By appropriate separation into a nonlinear and a linear subnetwork, large time constants (originating for example from feedback loops or bias networks) may be eliminated. As a result, the differences between the time constants are smaller, and the stiffness of the system is reduced considerably. If we treat the whole network totally in the time domain, the linear subnetwork does not exist, and therefore the term $\boldsymbol{D}(\boldsymbol{x})\boldsymbol{l}(t)$ in Eq. (84) vanishes and we obtain

$$\dot{\boldsymbol{x}} = \boldsymbol{A}(\boldsymbol{x})\boldsymbol{x} + \boldsymbol{B}(\boldsymbol{x})\boldsymbol{w}(\boldsymbol{x}) = \boldsymbol{F}(\boldsymbol{x}) \tag{86}$$

The nonlinear oscillator subnetwork is described by Eqs. (84) and (85). In addition to the periodic boundary condition $\boldsymbol{x}(t) = \boldsymbol{x}(t + T^0)$, the voltages and currents of $\boldsymbol{c}(t)$ and $\boldsymbol{c}'(t)$ must coincide. $\boldsymbol{c}'(t)$ may be expressed by

$$\boldsymbol{c}'(t) = \int_{-\infty}^{+\infty} \boldsymbol{V}(t)\boldsymbol{l}(t - t_1)\,dt_1 = \boldsymbol{V}(t) * \boldsymbol{l}(t) \tag{87}$$

where $\boldsymbol{V}(t)$ is the impulse response of the linear subnetwork. As in the previous section we normalize the time variable with respect to $T^0$ and obtain

$$\frac{d\boldsymbol{x}}{d\tau} = (\boldsymbol{A}\boldsymbol{x} + \boldsymbol{B}\boldsymbol{w} + \boldsymbol{D}\boldsymbol{l})T^0, \quad \frac{dT^0}{d\tau} = 0, \qquad \tau = tT^0 \tag{88}$$

Since the oscillator signals are assumed to be periodic, it is possible to represent the port variables $\boldsymbol{l}(t)$ by periodic Fourier series,

$$\boldsymbol{l}(t) = \sum_{\nu=-\infty}^{+\infty} (\boldsymbol{l}_{r\nu} + j\boldsymbol{L}_{i\nu})e^{j2\pi\nu z} \tag{89}$$

From Eq. (87) we obtain

$$\boldsymbol{c}'(t) = \sum_{\nu=-\infty}^{+\infty} \boldsymbol{V}_\nu(\boldsymbol{l}_{r\nu} + j\boldsymbol{l}_{i\nu})e^{j2\pi\nu z} \tag{90}$$

where $\boldsymbol{V}_\nu$ is the hybrid matrix of the linear multiport, at the $\nu$th harmonic, which can be computed with standard linear network analysis methods. The Fourier series expansion representing the port variables is truncated after the $k$th element. In this case, due to the sampling theorem, it is necessary and sufficient that the condition $\boldsymbol{c}(t) = \boldsymbol{c}'(t)$ be fulfilled for $2K + 1$ discrete time values within the interval $T^0$). We obtain

$$\boldsymbol{c}(\tau_\nu) = \boldsymbol{c}'(\tau_\nu), \quad \tau_\nu = \frac{\nu - 1}{2K + 2}, \quad \nu = 1, 2, \ldots, 2K + 1 \tag{91}$$

The solution of Eq. (91) and the periodic boundary condition may be expressed, as in the subsection "Time-Domain Method as the solution of a boundary-value problem. The state equations of the nonlinear subnetwork are therefore supplemented by (2K + 1)$M$ additional state equations

$$\begin{aligned} \dot{\boldsymbol{x}} &= [\boldsymbol{A}(\boldsymbol{x})\boldsymbol{x} + \boldsymbol{B}(\boldsymbol{x})\boldsymbol{w}(\boldsymbol{x}) + \boldsymbol{D}(\tau)\boldsymbol{l}(\tau)]T^0 \\ \dot{T}_p &= 0 \\ \dot{L}_0 &= 0 \\ \dot{L}_1 &= 0 \\ &\vdots \\ \dot{L}_k &= 0 \end{aligned} \tag{92}$$

The required $n + (2K + 1)m$ boundary conditions are

$$\begin{aligned} \boldsymbol{c}(\tau_\nu) - \boldsymbol{c}'(\tau_\nu) &= 0, \qquad \tau_\nu = \tfrac{\nu-1}{2K+2}, \qquad \nu = 1, 2, \ldots, 2K + 1 \\ \boldsymbol{x}(0) - \boldsymbol{x}(1) &= 0 \end{aligned} \tag{93}$$

Notice that the boundary conditions are no longer only given at $\tau = 0$ and $\tau = 1$, but at $2K + 2$ points $\tau = (\nu-1)/(2K + 2)$, $\nu = 1, \ldots, 2K + 2$. Because of the special structure of the boundary-value problem the multiple-shooting algorithm can be adapted in a numerically efficient way (43).

## Noise in Oscillators

**Problems in Microwave Oscillator Noise Analysis.** Noise analysis of microwave oscillators is usually based on the assumption that the unperturbed state of the oscillator is almost sinusoidal. This allows the application of a describing-function method for the characterization of the nonlinear devices in the oscillator (51). Based upon this method, the noise behavior of microwave oscillators has been analyzed by Spälti (52), Edson (53) and Kurokawa (54,55). These methods have been applied and extended to special cases (56,57,58).

The above methods provide a good qualitative and to some extent also a quantitative description of the oscillator noise behavior. However, their applicability is restricted to simplified oscillator models, since their accuracy depends on the validity of the approximation of the dynamic behavior of the nonlinear elements by a describing function (55). Another severe limitation is that the upconversion of low-frequency noise such as $1/f$ noise cannot be treated by these methods.

Kärtner has developed a time-domain method for noise analysis of oscillators, based on the solution of the Langevin equations (59, 60). Adding the noise terms to the normal-form equations (69) yields

$$\frac{dx}{dt} = f(x, \xi, y_1, \ldots, y_M), \qquad x \in IR^N, \quad \xi \in IR^k \tag{94}$$

The vector $\xi$ describes white noise sources, and $y_1, \ldots, y_M$ represent $f^{-\alpha}$ noise sources. Colored noise sources may be derived from white noise sources by inserting linear systems transforming the white noise sources to colored noise. For considering $f^{-\alpha}$ noise sources infinite-dimensional systems are required. However, as shown in Ref. 60, these infinite-dimensional systems may be treated with analytical formulas, so that $f^{-\alpha}$ noise sources may be treated with low computational effort. Using the perturbation method, the correlation spectra of the phase and amplitude noise due to white noise sources as well as due to $f^{-\alpha}$ noise sources can be calculated. The method has been applied to bipolar transistor oscillators (59,60), to planar integrated microwave oscillators (61,62), and to varactor tunable oscillators (63).

Frequency-domain noise analysis can be performed on the basis of the harmonic balance method (64,65, 66). Starting from the harmonic balance equations (70), we obtain a nonlinear system of equations

$$F(X, \omega, N_T) = 0, \qquad X_T \in \mathbb{C}^{n(2k+1)}, N_T \in \mathbb{C}^{r(2k+1)} \tag{95}$$

In this equation $X_T$ is the system state vector summarizing the signal spectra of $n$ signals at a frequency $\omega$ close to the fundamental frequency $\omega_0$ and at $k$ harmonics. The subscript $T$ denotes that the signals are time-windowed (67,68). The vector $N_T$ summarizes the $r$ noise-source spectra at a frequency $\omega$ and at $\kappa$ harmonics. The numerical solution of this equation is based on correlation-matrix techniques.

Combining time- and frequency-domain techniques is also possible in noise analysis (69). The phase noise is computed in the time domain. The linear subcircuits are described by noise multiports. This method again exhibits the advantages of the time–frequency-domain method.

In Ref. 66 the results of measurements on designed and fabricated integrated oscillators are compared with numerical simulations based on the methods discussed above. Furthermore that paper considers a method to minimize oscillator phase noise by numerical optimization. Based on the computation of the oscillator steady-state and spectral behavior in the time domain, single-sideband phase noise is minimized using a method for optimal-control problems, a direct collocation algorithm (69,70)

Another essential requirement is the simulation of the startup behavior of oscillators. If the resonator is weakly damped, it is well known that many oscillations occur on the way to the steady state. Although some analytical results are available [see e.g. Rusznyak (71). where a simplified model of a crystal oscillator is used, the corresponding simulation problem is very complicated [see Schmidt-Kreusel (72)]. Recently Schmidt-Kreusel published an efficient solution for this problem, which is based on the idea that the transient trajectory of a weakly damped oscillator consists of nearly closed trajectories in the state space. If only a few parts of this transient are approximated by periodic solutions, the envelope of the transient behavior can be calculated in a fast manner. This approach is described in detail by Mathis (73). Recently, an alternative approach was published by Brachtendorf and Laur (74) that uses a certain kind of partial differential equations for calculating the envelope.

**Description of Noisy Circuits.** In linear noisy circuits we usually have to deal with stationary Gaussian noise signals. Such signals may be characterized completely by their correlation spectra (75). For a signal

$s(t)$ unlimited in time, the average power within the time interval of length $2T$ centered around $t$ is given by

$$\frac{1}{2T}\int_{t-T}^{t+T} |s(t_1)|^2 \, dt_1 \tag{96}$$

If for large time intervals $2T$ the average power approaches a limit, which is independent of $t$, the signal $s(t)$ is called stationary. The average power $\langle P \rangle$ of a stationary signal can be exactly defined by

$$\langle P \rangle = \lim_{T\to\infty} \frac{1}{2T}\int_{-T}^{+T} |s(t)|^2 \, dt \tag{97}$$

We investigate the more general function

$$c_{ij}(\tau) = \lim_{T\to\infty} \frac{1}{2T}\int_{-T}^{+T} s_i(t) s_j^*(t-\tau) \, dt \tag{98}$$

Which is called a *correlation function*. For $i = j$, the function $C_{ii}(\tau)$ is the *autocorrelation function* of the signal $s_i$(t) and for $i \neq j$ we have the *cross-correlation function* $C_{ij}(\tau)$ of the signals $s_i(t)$ and $s_j(t)$. With the time-windowed function $s_T(t)$ of the signal $s(t)$ defined by

$$s_T(t) = \begin{cases} s(t) & \text{for} \quad |t| \leq T \\ 0 & \text{for} \quad |t| > T \end{cases} \tag{99}$$

we can write Eq. (98) in the form

$$c_{ij}(\tau) = \lim_{T\to\infty} \frac{1}{2T}\int_{-\infty}^{+\infty} s_{iT}(t) s_{jT}^*(t-\tau) \, dt \tag{100}$$

The average power $\langle P \rangle$ of the signal $S_i(t)$ is given by

$$\langle P \rangle = c_{ii}(0) \tag{101}$$

We denote the Fourier transform of the time-windowed function $s_{iT}(t)$ by $S_{iT}(f)$:

$$s_{iT}(t) \circ\!\!-\!\!\bullet\, S_T(f) \tag{102}$$

As mentioned before, the symbol represents the correspondence between a pair of Fourier transforms. From Eq. (102), we obtain

$$s_{iT}(t) * s_{jT}^*(-t) \circ\!\!-\!\!\bullet\, S_{iT}(f) S_{jT}^*(f) \tag{103}$$

The symbol $*$ denotes the convolution operation

$$s_1(t) * s_2(t) = \int_{-\infty}^{+\infty} s_1(t_1) s_2(t - t_1)\, dt_1 \tag{104}$$

The correlation spectrum $C_{ij}(f)$, given by

$$C_{ij}(f) = \lim_{T \to \infty} \frac{1}{2T} S_{iT}(f) S_{jt}^*(f) \tag{105}$$

is the Fourier transform of the correlation function:

$$c_{ij}(\tau) \circ\!\!-\!\!\bullet\, C_{ij}(f) \tag{106}$$

$C_{ii}(f)$ with $i \neq j$ is the autocorrelation spectrum of the signal $s_i(t)$ and $C_{ii}(f)$ with $i = j$ is the cross-correlation spectrum of the signals $s_i(t)$ and $s_j(t)$. With the exception of a dimensional factor, $C_{ii}(f)$ is a spectral power density or a power spectrum. Since the autocorrelation function is a real and even function of $\tau$, the autocorrelation spectrum is a real and even function of frequency.

The cross-correlation function is complex. Changing the sign of the frequency or interchanging the indices $i$ and $j$ yields its complex conjugate.

$$2C_{ii}(f)\Delta f \tag{107}$$

The factor 2 results from considering both the positive- and negative-frequency parts. In general for random signals no amplitude spectra exist, whereas power spectra may be calculated even for random signals.

For a stationary noise signal $s_{ni}(t)$ the Fourier integral does not exist. However, a correlation function

$$c_{ij}(\tau) = \lim_{T \to \infty} \frac{1}{2T} \int_{-\infty}^{+\infty} \langle s_{niT}(t) s_{njT}^*(t - \tau) \rangle dt \tag{108}$$

can be defined, in which the brackets indicate the statistical mean over signals measured on an ensemble of identical circuits. If the signals $s_{ni}(t)$ and $s_{nj}(t)$ have zero mean, in general, the mean of the product $s_{ni}(t) s_{nj}{}^*(t - \tau)$ approaches 0 with arbitrary order for $\tau \to \infty$, so that the integral (108) and also its Fourier transform exist. Since the Fourier integral of a time-windowed function exists in general, the correlation spectrum may also be defined by

$$c_{ij}(f) = \lim_{T \to \infty} \frac{1}{2T} \langle s_{niT}(f) s_{njT}^*(f) \rangle \tag{109}$$

In this case, $T \to \infty$ has to be carried out after the ensemble averaging. The autocorrelation and cross-correlation spectra $C_{ij}(f)$ of the noise sources of a linear network are given by

$$C_{ij}(f) = \lim_{T \to \infty} \frac{1}{2T} \langle S_{iT}(f) S_{jT}^*(f) \rangle \tag{110}$$

where $S_{iT}(t)$, $S_{jT}(t)$ are the spectra of the time-windowed signals of the noise sources. The correlation spectra $C_{ij}(f)$ can be combined in the correlation matrix

$$\boldsymbol{C}(f) = \begin{bmatrix} C_{11}(f) & C_{12}(f) & \cdots & C_{1n}(f) \\ C_{21}(f) & C_{22}(f) & \cdots & C_{2n}(f) \\ \vdots & \vdots & & \vdots \\ C_{n1}(f) & C_{n2}(f) & \cdots & C_{nn}(f) \end{bmatrix} \tag{111}$$

The correlation matrix $C(f)$ can be represented as the product of the column vector

$$\boldsymbol{S_T}(\boldsymbol{f}) = \begin{bmatrix} S_{1T}(f) \\ \vdots \\ S_{nT}(f) \end{bmatrix} \tag{112}$$

and its Hermitian conjugate row vector

$$\boldsymbol{S}_T^{\dagger}(f) = \begin{bmatrix} S_{1T}^{*}(f) & \cdots & S_{nT}^{*}(f) \end{bmatrix} \tag{113}$$

in matrix notation by

$$\boldsymbol{C}(f) = \lim_{T\to\infty} \frac{1}{2T} \langle \boldsymbol{S}_T(f) \boldsymbol{S}_T^{\dagger}(f) \rangle \tag{114}$$

We now formally use the complex amplitudes $S_{iT}(f)$ in the same way as the amplitudes of deterministic signals. $S_{iT}(f)$ is the spectrum of a time-windowed noise signal. We can measure the noise signal within some finite interval of time, and we may calculate the spectrum of this sample. This specific sample of a noise signal has to be considered as a deterministic signal, since we have exact knowledge of its time dependence. The transition from deterministic signals to random signals is carried out in our description by performing the ensemble average. After doing so, in the case of random signals, the decomposition of the correlation matrix into a product of a column vector and a row vector will be impossible. For example in the case of a signal vector describing independent random noise sources, the nondiagonal elements will be averaged out to zero and the correlation matrix will be diagonal.

In general, the network equations have the following form in matrix notation:

$$\tilde{\boldsymbol{S}}_T(f) = \boldsymbol{M}(f)\, \boldsymbol{S}_T(f) \tag{115}$$

The coefficient matrix $\boldsymbol{M}(f)$ combines the complex amplitude vectors $\boldsymbol{S}_T(f)$ and $\boldsymbol{S'}_T(f)$. Multiplying Eq. (115) on the right by its Hermitiean conjugate, we obtain

$$\tilde{\boldsymbol{S}}_T(f) \tilde{\boldsymbol{S}}_T^{\dagger}(f) = \boldsymbol{M}(f)\, \boldsymbol{S_T}(\boldsymbol{f})\, \boldsymbol{S}_T^{\dagger}(f)\, \boldsymbol{M}(f)^{\dagger}(f) \tag{116}$$

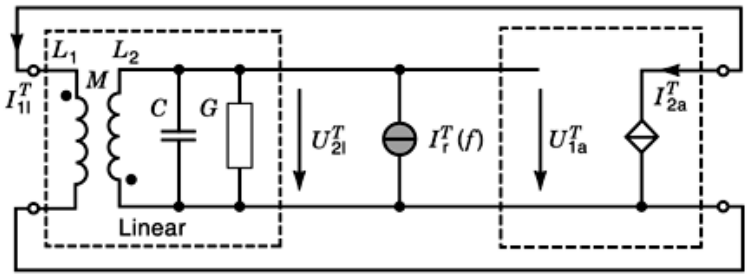


**Fig. 13.** Noisy two-port oscillator.

Evaluating the ensemble average on both sides and subsequently carrying out the transition $T \to \infty$ we obtain

$$\check{\boldsymbol{C}} = \boldsymbol{M}(f)\,\boldsymbol{C}(f)\,\boldsymbol{M}^{\dagger}(f) \tag{117}$$

This establishes a general rule for deriving equations for the correlation matrices from linear equations for the signal amplitudes. A linear noisy two-port may be characterized by two equivalent noise sources. These sources may be located at the input or at the output. If both sources are located at the same port, one must be a voltage source in series with the port and the other must be a current source in parallel with the port. If one equivalent noise source is assigned to every port, in general we may choose an equivalent current source or an equivalent voltage source at each port.

**Noise in Two-Port Oscillators.** We analyze the noise behavior of the simple two-port oscillator shown in Fig. 13. The left two-port is the linear frequency-determining feedback two-port. In our example the feedback network of the Meissner oscillator was chosen. The right two-port is the nonlinear amplifying two-port. In our example, all internal noise sources of the linear two-port as well as the nonlinear two-port are summarized in the noise current source $I_T{}^r(f)$. This equivalent noise source is obtained in the following way: In the first step, describe the noise properties of the linear feedback two-port by an equivalent output noise located at its output, and the noise properties of the active two-port by equivalent noise sources located at its input. To extract the noise parameters of the active two-port, we consider it to be linear. After connecting the output of the feedback two-port to the input of the active two-port, we can contract the four equivalent noise sources into one noise source $I_T{}^r(f)$.

For the oscillator circuit depicted in Fig. 13 the following equations are valid:

$$I_{1lT}(f) = A_{21}(f)V_{2lT}(f) + A_{22}(f)I_T^r(f) \tag{118}$$

$$I_{2aT}(f) = S(V)V_{1aT}(f) \tag{119}$$

$$V_{1aT}(f) = V_{2lT}(f) \tag{120}$$

$$I_{1lT}(f) = -I_{2aT}(f) \tag{121}$$

The variables $I_{1|T}(f)$, $V_{2|T}(f)$, $V_{1aT}(f)$ and $I_{2aT}(f)$ are the noise current and voltage amplitudes at the ports of the two-ports. To investigate of the oscillator noise behavior we have to consider the nonlinear saturation properties of the active two-port. $A_{21}(f)$ and $A_{22}(f)$ are circuit parameters of the feedback two-port in chain representation. In our simple model we describe the active element by a nonlinear voltage-controlled current source. With the real amplitude $V$ of the oscillator signal at the input of the nonlinear two-port we describe the relation between input and output noise signals by the amplitude-dependent transconductance $S(V)$. From Eqs. (118) to (121) we obtain

$$[A_{21}(f) + S(V)]\, V_{2|_T}(f) + A_{22}(f) I_T^r(f) = 0 \tag{122}$$

The autocorrelation spectra $C^I(f)$ and $C^V(f)$ of the noise current source $I^r{}_T(f)$ and the voltage current source $V^r{}_T(f)$ are given by

$$C^I(f) = \lim_{T\to\infty} \frac{1}{2T} \langle I_T^r(f) I_T^{r*}(f) \rangle \tag{123}$$

$$C^V(f) = \lim_{T\to\infty} \frac{1}{2T} \langle V_{2|T}(f) V_{2|T}^*(f) \rangle \tag{124}$$

With Eq. (122) we obtain

$$C^V(f) = \frac{|A_{22}(f)|^2}{|A_{21}(f) + S(V)|^2}\, C^I(f) \tag{125}$$

For the Meissner oscillator the circuit parameters of the linear feedback two-port are given by

$$A_{21}(f) = -G_0 \left[ 1 + jQ \left( \frac{f}{f_0} - \frac{f_0}{f} \right) \right] \tag{126}$$

$$G_0 = \frac{L_2}{|M|}\, G \tag{127}$$

$$Q = \frac{2\pi f_0 C}{G} \tag{128}$$

$$A_{22}(f) = -\frac{L_2}{|M|} \tag{129}$$

where $M$ is the mutual inductance of the transformer and $L_2$ is the inductance of the secondary coil. Substituting into Eq. (125), we obtain

$$C^V(f) = \left(\frac{L_2}{|M|}\right)^2 \frac{C^I(f)}{(G_0 - S)^2 + G_0^2\, Q^2\, (f/f_0 - f_0/f)^2} \tag{130}$$

The power spectral density at the load conductance $G$ is

$$W(f) = 2\, C^V(f)\, G \tag{131}$$

and the total power flowing into $G$ is given by

$$\overline{P}_0 = \int_0^{+\infty} C^V(f)\, G\, df \tag{132}$$

With

$$\int_{-\infty}^{+\infty} \frac{dx}{a^2 + b^2(x - 1/x)^2} = \frac{\pi}{ab} \tag{133}$$

we obtain

$$\overline{P}_0 = \pi \frac{f_0\, C^I}{Q(G_0 - S)} \tag{134}$$

The frequency deviation $\Delta f$ from the carrier is given by $\Delta f = f - f_0$. For $\Delta f << f_0$ we can approximate

$$\frac{f}{f_0} - \frac{f_0}{f} \approx 2\frac{\Delta f}{f_0} \tag{135}$$

To characterize the oscillator noise we introduce the *noise measure* $M_r$. The noise measure is the factor by which the power spectral density of a noise source exceeds the thermal noise. The autocorrelation spectrum of the equivalent noise source of a conductance $G$ exhibiting thermal noise at a temperature $T$ is given by $2kTG$. From this definition it follows that

$$M_r = \frac{C^I}{2\, kTG} \tag{136}$$

From Eqs. (130), (131), (135), and (136) we obtain the power spectral density of the oscillator,

$$W(f) = \frac{4\, kTM_r G_0^2}{(G_0 - S)^2 + 4\, G_0^2 Q^2\, (\Delta f/f_0)^2} \tag{137}$$

From Eqs. (132) and (136) we obtain the average total power

$$\overline{P}_0 = \frac{2\pi k T_0 M_r G f_0}{Q(G_0 - S)} \tag{138}$$

We define the spectral width of the oscillator as the ratio of the average power $\bar{P}_0$ to the power spectral density $W(f_0)$ at the center frequency $f_0$,

$$B = \frac{\overline{P}_0}{W(f_0)} \tag{139}$$

and obtain

$$B = \pi \frac{G_0 - S}{G_0} \frac{|M|}{L_2} \frac{f_0}{Q} \tag{140}$$

In the oscillator without noise, $S$ equals $G_0$, whereas in the noisy case we have $G_0 - S > 0$. The oscillator amplitude is determined by the nonlinear gain characteristics of the active element. It is only slightly influenced by the noise source. The ratio $G_0/(G_0 - S)$ is determined by the ratio of the saturation power $\bar{P}_0$ to the injected noise power. Using Eq. (138), we can express $G_0 - S$ the ratio of the power spectral density of the equivalent noise source to the saturation power of the oscillator and obtain

$$B = \frac{2\pi^2 f_0^2}{Q^2} \left( \frac{|M|^2}{L_2} \right) \frac{kTM_r}{\overline{P}_0} \tag{141}$$

The spectral width of the oscillator is directly proportional to the noise measure $M_r$, and inversely proportional to the reciprosal saturation power and to the square of the quality factor $Q$ of the resonant circuit. Low-noise design of oscillators requires a low-noise active element, a high quality factor of the active circuit, and a high saturation power of the oscillator. Since the amplitude of the oscillator is stabilized by the nonlinear saturation behavior of the oscillator, an oscillator exhibits primarily amplitude noise.

**Noise Analysis in the Frequency Domain.** In the following a frequency-domain perturbation method for simulating the noise behavior of free-running microwave oscillators is presented (66). The method is based on a piecewise harmonic balance technique. The single-sideband phase noise of the oscillator is derived from the system equations. The method is limited neither to certain circuit topologies nor to certain types of noise sources.

*Fluctuations of the State Variables.* In the frequency-domain method, noise sources may be considered by extending the nonlinear system of equations (82). Introducing the noise source vector $\boldsymbol{N}_T(\omega)$, which summarizes the time-windowed spectra of the noise sources, the system equations now exhibit the following form:

$$\boldsymbol{F}(\boldsymbol{X}_T, \omega, \boldsymbol{N}_T) \equiv \boldsymbol{0} \tag{142}$$

The index $T$ denotes the time-windowed signal spectra as defined in Eq. (102). The vector $\boldsymbol{N}_T \epsilon \, C^{r(2k+1)}$ summarizes the amplitudes at the fundamental frequency $\omega_0$ and at the harmonics up to $K\omega_0$ of a number $r$ of noise sources of arbitrary spectrum. In Eq. (142) all harmonics up to $k^{\text{th}}$ order and their fluctuations are considered.

This allows us to compute the complete correlation spectrum at the frequency deviation $\omega_m = \omega - \omega_0$. All noise processes, including the upconversion of low-frequency noise, are considered. Since the noise contribution is small compared with the deterministic part of the oscillator signal, the noise contribution may be considered as a first-order perturbation. From Eq. (142) we obtain

$$\boldsymbol{F}(\boldsymbol{X}_T, \omega) + \boldsymbol{G}(\boldsymbol{X}_T^0, \omega)\, \boldsymbol{N}_T = \boldsymbol{0} \tag{143}$$

with $\boldsymbol{G}(\boldsymbol{X}^0{}_T, \omega) \in C^{n(2k+1)\times r(2k+1)}$ and

$$\boldsymbol{G}(\boldsymbol{X}_T^0, \omega) \equiv \left.\frac{\partial \boldsymbol{F}(\boldsymbol{X}_T, \omega)}{\partial \boldsymbol{N}_T}\right|_{\boldsymbol{X}_T = \boldsymbol{X}_T^0, \boldsymbol{N}_T = \boldsymbol{0}} \tag{144}$$

The matrix $\boldsymbol{G}(\boldsymbol{X}^0{}_T, \omega)$ describes the coupling of the noise sources $\boldsymbol{N}_T$ with the system. It is assumed that noise sources effect only a small perturbation of the limit cycle of the oscillator:

$$\begin{aligned} \boldsymbol{X}_T(\omega) &= \boldsymbol{X}_T^0(\omega) + \delta \boldsymbol{X}_T(\omega), \quad \omega = \omega_0 + \omega_m, \\ \| \delta \boldsymbol{X}_T(\omega) \| &\ll \| \boldsymbol{X}_T^0(\omega) \|, \qquad \omega_m \ll \omega_0 \end{aligned} \tag{145}$$

Therefore the system of nonlinear equations (143) may be linearized in the neighborhood of the limit cycle, and we obtain

$$\boldsymbol{J}(\boldsymbol{X}_T^0, \omega)\delta \boldsymbol{X}_T + \boldsymbol{G}(\boldsymbol{X}_T^0, \omega)\boldsymbol{N}_T = \boldsymbol{0} \tag{146}$$

with the Jacobian matrix $\boldsymbol{J}(\boldsymbol{X}^0{}_T, \omega) \in C^{n(2k+1)\times n(2k+1)}$ of the unperturbed system equations given by

$$\boldsymbol{J}(\boldsymbol{X}_T^0, \omega) \equiv \left.\frac{\partial \boldsymbol{F}(\boldsymbol{X}_T, \omega, 0)}{\partial \boldsymbol{X}_T}\right|_{\boldsymbol{X}_T = \boldsymbol{X}_T^0} \tag{147}$$

This equation describes the perturbation of the oscillator by the noise sources. It includes the mixing of the injected noise signals $\boldsymbol{N}_T$ with the unperturbed state variables $\boldsymbol{X}_T{}^0$. From the solution of the linearized system of equations (146) the correlation spectra of the state variables may be computed.

A problem arises from the fact that the Jacobian matrix $\boldsymbol{J}(\boldsymbol{X}^0{}_T, \omega_0)$ is singular for the limit cycle of the unperturbed system (35,76) The linearized perturbed system equations cannot be solved by inversion or by $LR$ decomposition. The smallest eigenvalue of the Jacobian is $\lambda_1 = 0$. A perturbation $\delta \boldsymbol{X}_T$ corresponding to the eigenvalue 0 of the Jacobian induces a perturbed solution $\boldsymbol{X}^0{}_T + \delta \boldsymbol{X}_T$, which is again a solution of the system equations (142). The eigenvector corresponding to the eigenvalue $\lambda_1 = 0$ is tangent to the limit cycle. The fluctuations in direction of this eigenvector are the phase fluctuations. The subspace spanned by the other eigenvectors of the Jacobian is the space of the amplitude fluctuations. This subdivision of the eigenvector space of the Jacobian allows a clear and well-defined distinction between phase and amplitude fluctuations.

*Solution of the System Equations Including Noise.* The Jacobian is singular at the steady state, and for a small frequency deviation $f_m$ of the carrier frequency the deviations of the matrix elements are small and the condition number of the Jacobian remains high (76). The condition number cond, defined by

$$\text{cond}\ (\boldsymbol{J}) = \|\boldsymbol{J}\|\, \|\boldsymbol{J}^{-1}\| \tag{148}$$

provides a measure for the numerical error in the solution of a linear system of equations (77, 50). Here $\|\boldsymbol{J}\|$ is the matrix norm of the Jacobian $\boldsymbol{J}$. The condition number of a matrix may be approximated by the ratio of its largest to its smallest eigenvalue (77). The largest eigenvalue is much larger than the frequency of oscillation $f_0$, because it is related to the fastest process of the system. The smallest eigenvalue is of the order of the frequency deviation $f_\mathrm{m}$, as we will show later in Eq. (166). Therefore the condition number cond of the Jacobian is much larger than the ratio of the carrier frequency to the frequency deviation of interest (78):

$$\mathrm{cond}\ \left(\boldsymbol{J}(\boldsymbol{X}_T^0, 2\pi(f_0 + f_\mathrm{m}))\right) \gg \frac{f_0}{f_\mathrm{m}} \tag{149}$$

This means that the steady state of an oscillator has to be determined to a much higher precision than the reciprol of the condition number to achieve a relative error smaller than 1 (50). Considering a 10 GHz oscillator and a frequency deviation of say, $f_\mathrm{m} = 10$ kHz, the condition number is much larger than $10^6$. To overcome the numerical problems the Jacobian is linearized at the carrier frequency with respect to the frequency:

$$\boldsymbol{J}(\boldsymbol{X}_T^0, \omega) = \boldsymbol{J}(\boldsymbol{X}_T^0, \omega_0) + \omega_m\, \boldsymbol{J}_\omega(\boldsymbol{X}_T^0, \omega_0) \tag{150}$$

with the abbreviation

$$\boldsymbol{J}_\omega(\boldsymbol{X}_T^0, \omega_0) \equiv \left.\frac{\partial \boldsymbol{J}(\boldsymbol{X}_T^0, \omega)}{\partial \omega}\right|_{\omega=\omega_0} \tag{151}$$

An eigenvalue decomposition (77) of the Jacobian with left- and right-side eigenvectors is used. Thus the complete correlation spectra can be calculated in a numerically stable way. First we want to analyze the unperturbed Jacobian $\boldsymbol{J}_\omega(\boldsymbol{X}^0{}_T, \omega_0)$. The left- and right-side eigenvectors of the Jacobian are denoted by $\boldsymbol{V}^\dagger{}_j$ and $\boldsymbol{W}_i$, and the eigenvalues by $\lambda^V{}_j$ and $\lambda^W{}_j$ respectively. We have

$$\boldsymbol{V}_j^\dagger\, \boldsymbol{J}(\boldsymbol{X}_T^0, \omega_0) \;=\; \lambda_j^V\, \boldsymbol{V}_j^\dagger, \qquad \boldsymbol{V}_j \in C^{n(2k+1)} \tag{152}$$

$$\boldsymbol{J}(\boldsymbol{X}_T^0, \omega_0)\, \boldsymbol{W}_i \;=\; \lambda_i^W\, \boldsymbol{W}_i, \qquad \boldsymbol{W}_i \in C^{n(2k+1)} \tag{153}$$

The eigenvalues of the Jacobian are equal for a set of left- and right-side eigenvectors:

$$\lambda_j^V = \lambda_i^W = \lambda_i \qquad \text{for} \qquad i = j \tag{154}$$

The left- and right-side eigenvectors satisfy the orthogonality relations (76)

$$\boldsymbol{V}_j^\dagger\, \boldsymbol{W}_i = \delta_{ij} \qquad \text{with} \qquad \delta_{ij} = \begin{cases} 1, & i = j \\ 0, & i \neq j \end{cases} \tag{155}$$

According to these equations, the eigenvector $\boldsymbol{V}_1$ is orthogonal to all right-side eigenvectors $\boldsymbol{W}_i$ with the exception of $\boldsymbol{W}_1$. The eigenvectors corresponding to the eigenvalue $\lambda_1 = 0$ are denoted by $\boldsymbol{V}_1$ and $\boldsymbol{W}_1$. These eigenvectors will be investigated in the following in detail.

The eigenvector $\boldsymbol{W}_1$ is determined by the steady-state solution (64,79):

$$\boldsymbol{W}_1 = j\omega_0 \boldsymbol{K} \boldsymbol{X}_T^0 \tag{156}$$

where $\boldsymbol{K} \epsilon\, I\!R^{n(2k+1)\times n(2k+1)}$ is a matrix that has only nonvanishing diagonal elements consisting of the numbers of the harmonics:

$$\boldsymbol{K} = \begin{bmatrix} -k & & & & & & \\ & -(k-1) & & & & \mathbf{0} & \\ & & \ddots & & & & \\ & & & +k & & & \\ & & & & -k & & \\ & & & & & \ddots & \\ & \mathbf{0} & & & & & k \end{bmatrix} \tag{157}$$

Figure 14 illustrates the meaning of the eigenvectors $\upsilon_i(t)$ and $\omega_i(t)$ in the time domain. The vector $\upsilon_I(t)$ $\boldsymbol{V}_1(f)$ is the tangent vector to the steady-state limit cycle $\boldsymbol{x}^0(t)$, and $\omega_1$ $\boldsymbol{W}_1(f)$ is the normal vector defining a plane $N$ that is mapped onto itself by the unperturbed flux of the linearized set of differential equations (Poincaré map); see Ref. 60. The left-side eigenvector $\boldsymbol{V}_1$ is determined via

$$\boldsymbol{J}^\dagger(\boldsymbol{X}_T^0, \omega_0)\, \boldsymbol{V}_1 = \mathbf{0} \tag{158}$$

which is a linear homogeneous system of equations and can be solved with a standard $LU$ decomposition. The length of the vector $\boldsymbol{V}_1$ has to be normalized to satisfy, Eq. (155):

$$\| \boldsymbol{V}_1 \|_2 = \| \omega_0 \boldsymbol{K} X_T^0 \|_2^{-1} \tag{159}$$

The eigenvectors $\boldsymbol{W}_\mathrm{i}$ are a complete basis for the state space, and due to Eq. (155) a multiplication of $\boldsymbol{V}^\dagger{}_1$ with a vector within the state space is a projection onto the complementary space of the plane $N$. This means that the projection operator $\boldsymbol{W}_1\boldsymbol{V}^\dagger{}_1$ applied to any vector $\boldsymbol{z} = \Sigma^n{}_{i=1}\, a_i \boldsymbol{W}i$ results in a vector with a tangential component $a_1$ with respect to the limit cycle. So if this projection operator $\boldsymbol{W}_1\boldsymbol{V}^\dagger{}_1$ is applied to the noise sources in the state space $\boldsymbol{G}(\boldsymbol{X}^0T,\omega)\boldsymbol{N}_T$ the contributions of the noise sources that cause a phase shift of the unperturbed steady state are separated. This will be shown in the following. For a small frequency deviation $f_\mathrm{m}$ the deviations of the elements of the Jacobian are small. Therefore the deviations of the eigenvalues and eigenvectors of the Jacobian are small too (77):

$$\lambda_i' = \lambda_i + \delta\lambda_i, \qquad |\, \delta\lambda_i \,| \ll |\, \lambda_i \,| \tag{160}$$

$$\boldsymbol{V'}_j^\dagger = \boldsymbol{V}_j^\dagger + \delta \boldsymbol{V}_j^\dagger, \qquad \| \delta \boldsymbol{V}_j \|_2 \ll \| \boldsymbol{V}_j \|_2 \tag{161}$$

$$\boldsymbol{W'}_i = \boldsymbol{W}_i + \delta \boldsymbol{W}_i, \qquad \| \delta \boldsymbol{W}_i \|_2 \ll \| \boldsymbol{W}_i \|_2 \tag{162}$$

The eigenvalues and eigenvectors of the perturbed Jacobian $\boldsymbol{J}_\omega (\boldsymbol{X^0}_T, \omega_0)$ are denoted by a prime. It is sufficient to consider the deviations of the eigenvalues and eigenvectors up to the first order in $\omega_m$:

$$\delta\lambda_i = \omega_{\mathrm{m}} \boldsymbol{V}_i^\dagger \boldsymbol{J}_\omega(\boldsymbol{X}_T^0, \omega_0) \boldsymbol{W}_i \tag{163}$$

$$\delta \boldsymbol{W}_i = \sum_{l=1, l\neq i}^{n(2k+1)} \frac{\omega_{\mathrm{m}}}{\lambda_i - \lambda_l} \left[ \boldsymbol{V}_l^\dagger \boldsymbol{J}_\omega(\boldsymbol{X}_T^0, \omega_0) \boldsymbol{W}_i \right] \boldsymbol{W}_l \tag{164}$$

$$\delta \boldsymbol{V}_j = \sum_{l=1, l\neq j}^{n(2k+1)} \frac{\omega_{\mathrm{m}}}{\lambda_j - \lambda_l} \left[ \boldsymbol{V}_j^\dagger \boldsymbol{J}_\omega(\boldsymbol{X}_T^0, \omega_0) \boldsymbol{W}_l \right] \boldsymbol{V}_l \tag{165}$$

The eigenvalue $\lambda'_1$ is of special interest, since it is identical with the deviation $\delta\lambda_1$ from the lowest eigenvalue $\lambda_1 = 0$ of the unperturbed system. Using Eq. (156), we obtain

$$\lambda'_1 = \delta\lambda_1 = 2\pi f_{\mathrm{m}} \boldsymbol{V}_1^\dagger \boldsymbol{J}_\omega(\boldsymbol{X}_T^0, \omega_0) j 2\pi f_0 \boldsymbol{K} \boldsymbol{X}_T^0 \tag{166}$$

The smallest eigenvalue of the perturbed Jacobian $\lambda'_1 = \delta\lambda_1$ is therefore of the same order of magnitude as the small frequency deviation $\omega_m$. The inverse $\boldsymbol{J}^{-1}{}_\omega (\boldsymbol{X^0}_T, \omega_0)$ of the Jacobian is represented by an eigenvalue decomposition with the eigenvalues and left- and right-side eigenvectors of the Jacobian $\boldsymbol{J}_\omega (\boldsymbol{X^0}_T, \omega_0)$:

$$\boldsymbol{J}^{-1}(\boldsymbol{X}_T^0, \omega) = \sum_{i=1}^{n(2k+1)} \frac{1}{\lambda'_i} \boldsymbol{W'}_i \boldsymbol{V'}_i^\dagger \tag{167}$$

This inversion will not be performed, due to the ill-conditioning of the Jacobian. We have derived this equation only to calculate the correlation spectrum of the state-variable fluctuations. Later on we take into account the special eigenvalue $\lambda'_1$ that causes the ill-conditioning of the matrix and the problems associated with numerical inversion.

The state-variable fluctuations are given by

$$\delta \boldsymbol{X}_T = - \sum_{i=1}^{n(2k+1)} \frac{1}{\lambda'_i} \boldsymbol{W'}_i \boldsymbol{V'}_i^\dagger [\boldsymbol{G}(\boldsymbol{X}^0, \omega) \boldsymbol{N}_T] \tag{168}$$

*Correlation Spectrum of the Oscillator Noise.* The correlation spectra of the state variables $C^{\delta X}(f)$ and the noise sources $C^N(f)$ are given by

$$\boldsymbol{C}^{\delta X}(f) = \lim_{T\to\infty} \frac{1}{2T} \langle \delta \boldsymbol{X}_T(f) \delta \boldsymbol{X}_T^\dagger(f) \rangle \tag{169}$$

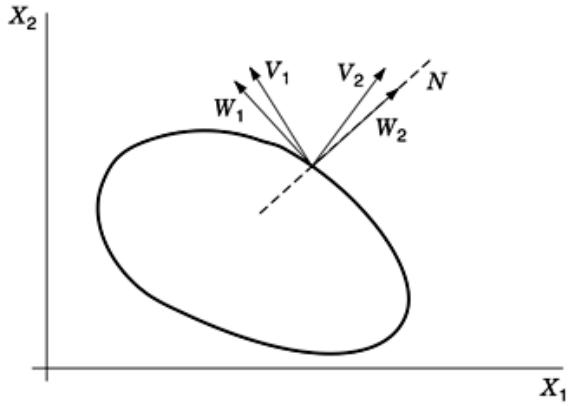


**Fig. 14.** Limit cycle in a two-dimensional phase space.

$$\boldsymbol{C}^N(f) = \lim_{T\to\infty} \frac{1}{2T} \langle \boldsymbol{N}_T(f) \boldsymbol{N}_T^\dagger(f) \rangle \tag{170}$$

where the brackets denote the ensemble average. The correlation spectra of the state variables are derived using Eqs. (169), (171) and the equation (168) of the state-variable fluctuations:

$$\boldsymbol{C}^{\delta X}(f) = \sum_{i=1}^{n(2k+1)} \sum_{j=1}^{n(2k+1)} \frac{1}{\lambda_i' \lambda_j'^*} \left[ \boldsymbol{V'}_i^\dagger \boldsymbol{C}^{GN}(f) \boldsymbol{V'}_j \right] \boldsymbol{W'}_i \boldsymbol{W'}_j^\dagger \tag{171}$$

with the abbreviation

$$\boldsymbol{C}^{GN}(f) = \boldsymbol{G}(\boldsymbol{X}_T^0, \omega) \boldsymbol{C}^N(f) \boldsymbol{G}^\dagger(\boldsymbol{X}_T^0, \omega) \tag{172}$$

The approximations Eqs. of (163), (164), and (165) for the eigenvalues and eigenvectors of the perturbed Jacobian are used to derive the correlation spectra of the state-variable fluctuations. The term with the major contribution to the correlation spectrum is the term with $i = j = 1$, due to the small eigenvalue $\lambda'_1 = \delta\lambda'_1$ given in Eqs. (27). This term represents, as already described, the phase noise of oscillators. As the perturbations of the eigenvectors $\delta \boldsymbol{W}_1$ and $\delta \boldsymbol{V}_1$ are of the order of $\omega_\mathrm{m}$ and therefore small compared with the unperturbed eigenvectors, they are negligible, and we have

$$\boldsymbol{C}^{\delta X}(f) = \frac{\left[ \boldsymbol{V}_1^\dagger \boldsymbol{C}^{GN}(f) \boldsymbol{V}_1 \right] \boldsymbol{K} X^0 \boldsymbol{X}^{0\dagger} \boldsymbol{K}}{(2\pi f_\mathrm{m})^2 |\boldsymbol{V}_1^\dagger \boldsymbol{J}_\omega(\boldsymbol{X}^0, \omega_0) \boldsymbol{K} X^0|^2}. \tag{173}$$

Due to the special situation of the eigenvalue $\lambda'_1$ and the eigenvectors $\delta \boldsymbol{W}_1$ and $\delta \boldsymbol{V}_1$, the terms with $i = 1$ and $j \neq 1$ or $i \neq 1$ and $j = 1$ in Eq. (171) represent the amplitude-phase correlation spectra. Finally, the terms

with $i \neq 1$ and $j \neq 1$ in Eq. (171) represent amplitude noise. These noise contributions are small compared with the phase noise, due to their larger eigenvalues, and are not taken into account in the following.

*Single-Sideband Phase Noise.* The single-sideband phase noise $\boldsymbol{L}(f_\mathrm{m})$ is the ratio of the noise power in a sideband of bandwidth 1 Hz at a frequency deviation $f_\mathrm{m} = f - f_0$ from the carrier frequency to the total signal power $\boldsymbol{P}_\mathrm{S}$. The value of $\boldsymbol{L}(f_\mathrm{m})$ is the same for all state variables, and therefore we can choose any state variable $x_i$ to calculate the single-sideband phase noise:

$$L(f_\mathrm{m}) = P_{Ni}(f_\mathrm{m})/P_{\mathrm{S}i} \tag{174}$$

In order to obtain the single-sideband phase noise at the fundamental frequency, the matrix element corresponding to the $i^{\mathrm{th}}$ state variable is chosen, which represents the noise power at the fundamental frequency. We have to select the element $|X^0{}_{i,1}|^2$ of the matrix $\boldsymbol{K}\boldsymbol{X}^0\boldsymbol{X}^{0\dagger}\boldsymbol{X}$ and obtain for the noise power $P_{Ni}\,(f_\mathrm{m})$ in a 1 Hz bandwidth

$$P_{Ni}(f_\mathrm{m}) = 2\boldsymbol{C}^{\,\delta X}(f_0 + f_\mathrm{m})_{i,1}\,R_\mathrm{n} = 2\frac{|X^0_{i,1}|^2 R_\mathrm{n}\,\boldsymbol{V}_1^\dagger \boldsymbol{C}^{GN}(f)\boldsymbol{V}_1}{(2\pi f_\mathrm{m})^2 |\boldsymbol{V}_1^\dagger \boldsymbol{J}_\omega(\boldsymbol{X}^0, \omega_0)\boldsymbol{K}X^0|^2} \tag{175}$$

Here $R_\mathrm{n}$ is a normalization resistance. The signal power of the fundamental frequency is represented by

$$P_{\mathrm{S}i} = 2|X^0_{i,1}|^2 R_\mathrm{n} \tag{176}$$

With the definition of the single-sideband phase noise in Eq. (174) we derive an equation for $L(f_\mathrm{m})$ using the approximations of the noise power (175) and the signal power (176):

$$L(f_\mathrm{m}) = \frac{1}{(2\pi f_\mathrm{m})^2} \cdot \frac{\boldsymbol{V}_1^\dagger \boldsymbol{C}^{GN}(f_0 + f_\mathrm{m})\boldsymbol{V}_1}{|\boldsymbol{V}_1^\dagger \boldsymbol{J}_\omega(\boldsymbol{X}^0, 2\pi f_0)\boldsymbol{K}X^0|^2} \tag{177}$$

where $V_1$ is the solution of the homogeneous linear system of equations

$$\boldsymbol{J}^\dagger(\boldsymbol{U}^0_T, 2\pi f_0)\boldsymbol{V}_1 = \boldsymbol{0} \tag{178}$$

which can be obtained very easily with a standard $LU$ decomposition of the Jacobian. The derivative of the Jacobian with respect to the frequency, $\boldsymbol{J}^\dagger{}_\omega(\boldsymbol{U}^0,\, 2\pi F_0)$, can be calculated numerically, as we will show in our example. The denominator of the second factor is constant for different frequency deviations and needs to be calculated only once. The numerator consists of the correlation spectrum of the noise sources multiplied by the vector $\boldsymbol{V}^\dagger{}_1$ on the left side and by $\boldsymbol{V}_1$ on the right side. As we already described, this multiplication is a projection of all noise sources of the state space onto the tangent vector to the steady state. That means the vector $\boldsymbol{V}_1$ selects the contributions of the noise sources that are tangential to the steady state and therefore induce phase noise. The noise sources ($1/f^\alpha$ noise and white noise and their modulation are taken into account in the correlation matrix $C^{GN}$. The correlation spectrum of a $1/f^\alpha$-noise source decreases at $10\alpha$ dB per frequency decade, and therefore $\boldsymbol{L}(F_\mathrm{m})$ decreases at $20 + 10\alpha$ dB per decade. The single-sideband phase noise decreases at 20 dB per decade due to white noise sources, because the correlation spectra of white noise sources are independent of frequency. This method results in a numerically stable calculation of the phase noise of

free-running oscillators, where all effects of the noise sources converted with harmonic signals are taken into account.

## Synchronization of Oscillators

In the previous sections electronic oscillators without excitation are considered but even in the early days of oscillators an undesired entrainment phenomena in forced oscillators was described by Möller (80) and others [see van der Pol (81) around 1920. Although van der Pol mentioned forced oscillations in his 1920 paper he only considered circuits with positive (differential) resistances. In 1922 Appleton (82) discussed "automatic synchronization" of forced triode oscillators (only another expression for entrainment), and in the following years this subject was studied in more detail [see van der Pol's review paper (83)], but a sound mathematical basis for entrainment phenomena was not presented until the paper of Andronov and Vitt (84)] in 1930, where again mathematical ideas of Poincaré were used. A modern presentation can be found for example in the monograph of Jordan and Smith (12). In 1945 Tucker emphasized (85), "The synchronization (or entrainment) of oscillators was originally investigated because of difficulties experienced with early radio transmitters of "pull-in" to adjacent-station frequencies. Since then, however, the properties of oscillators under the influence of injected tones have been utilized in several ways," and he mentioned ideas from his Ph.D. thesis about applications to carrier telephone systems, and Kirschstein's (86) miscellaneous applications in radio and other applications in communication engineering. Today many of these early applications of entrainment and synchronization of forced oscillators are discussed in the context of so-called phase-locked loops [see e.g. Stensby (87) for further details and references]. Although it seems that PLL circuits and forced electronic oscillators differ in their circuit structure, a mathematical analysis shows similar phenomena in both circuits.

In this section some aspects of entrainment will be illustrated using the forced van der Pol equation (with normalized $\omega^2{}_0 = 1$)

$$\ddot{x} + \varepsilon(x^2 - 1)\dot{x} + x = \Gamma \cos \omega t \tag{179}$$

where $\epsilon > 0$. Following Jordan and Smith (12), where van der Pol's idea is used, we look for responses approximately of the form

$$x(t) = a(t) \cos \omega t + b(t) \sin \omega t \tag{180}$$

where $a$, $b$ are slowly varying functions. Neglecting ä, $\ddot{b}$, we obtain after some calculations a system of differential equations for the amplitude functions $a$ and $b$:

$$(2\omega - \tfrac{1}{2}\varepsilon ab)\dot{a} + \varepsilon(1 - \tfrac{1}{4}a^2 - \tfrac{3}{4}b^2)\dot{b} = \varepsilon\omega a(1 - \tfrac{1}{4}r^2) - (\omega^2 - 1)b \tag{181}$$

$$-\varepsilon(1 - \tfrac{3}{4}a^2 - \tfrac{1}{4}b^2)\dot{a} + (2\omega + \tfrac{1}{2}\varepsilon ab)\dot{b} = (\omega^2 - 1)a + \varepsilon\omega b(1 - \tfrac{1}{4}r^2) + \Gamma \tag{182}$$

where $r^2 = a^2 + b^2$. The periodic solutions with the frequency $\omega$ of the input function $\Gamma \cos \omega t$ [r.h.s. of Eq. (179)] correspond to the equilibrium points ($\dot{a} = 0$, $\dot{b} = 0$) of these equations. Using the abbreviations $\nu = (\omega^2 - 1)/\epsilon\omega$ (detuning) and $\gamma = \Gamma/\epsilon\omega$, we obtain from the equilibrium equations the following condition for

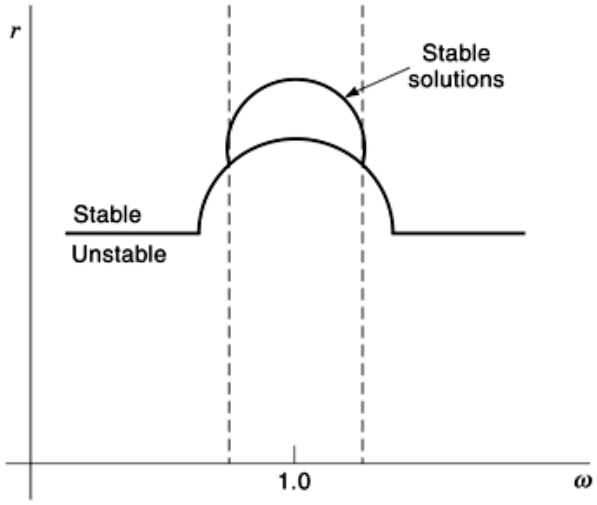


**Fig. 15.** Response Diagram of the van der Pol equation.

*response* solutions

$$r^2\left[\nu^2 + (1 - \tfrac{1}{4}r^2)^2\right] = \gamma^2 \qquad (183)$$

Analysis of this polynomial equation shows that there are one or three real roots (since $r > 2$), depending on the parameter values $\nu$ and $\gamma$. A graphical representation of $r^2$ in dependence on $|\nu|$ called the *response diagram* can be found for example, in Jordan and Smith (12). Based on these equilibrium points, a stability analysis has to be performed. As a conclusion it can be found that for certain values of the parameters $\nu$ and $\gamma$, around the frequency ${\omega^2}_0 = 1$ ($\nu = 0$) of the *free* oscillator (i.e. zero input function) there is a finite region (*lock-in band*) of detunings $\nu$ where a stable harmonic solution (with frequency $\omega$) exists. This region of frequencies corresponds to the region of entrainment or synchronization. Outside this region of frequencies there are no stable harmonic solutions with the input frequency $\omega$, and in the $a$–$b$ plane limit cycles appear. In Fig. 15 a variant of the response diagram is shown using the coordinates $r$ and $\omega$. A first curve subdivides the $r$–$\omega$ plane into stable and unstable areas, whereas the upper semicircle corresponds to the stable solutions of the polynomial equation (183). The dashed lines bound the entrainment or synchronization region. These results were first published by Andronov and Vitt (84).

Note, that the forced vdp equation is nonlinear, and in contrast to linear differential equations with constant coefficients, where general solutions are consist of a superposition of free and forced oscillations, this distinction makes no sense, although it seems obvious if the frequencies $\omega_0$ and $\omega$ are widely separated.

By means of the above mathematical concept some basic aspects of entrainment synchronization phenomena can be discussed, but there are other effects (e.g. higher harmonics, subharmonics) where more involved techniques have to be applied. The reader is referred to the monograph of Jordan and Smith (12) for further details. For the analysis of PLL circuits with feedback structure the monograph of Stensby (87) is very helpful.

Finally we should mention that there is a close relationship between synchronization and chaotic behavior. This subject is treated in an interesting paper of Tsang et al. (88) As a conclusion of their discussion it can be emphasized that each circuit with synchronization properties is a candidate for a chaotic system.

## Miscellaneous Problems of Oscillator Design

Besides the design problems discussed above, there are further problems that are essential in the design of oscillators. Some of these are mentioned here but the reader is referred to the literature; the monographs of Parzen (6), Frerking (89), and Kurz and Mathis (33) discuss many interesting design aspects. Several monographs are available that consider the design of microwave oscillators [e.g. Vendelin (90)]. We will discuss only some more general aspects of oscillator design. Most *spurious oscillations* are caused by the parastic inductances and capacitances in the active devices (e.g. transistors) or the physical layout of the components of the oscillator circuit. A main approach to avoid these oscillations is to introduce additional damping (e.g. additional resistors). Parasitics that are related to the layout and to poor design can be reduced only by an experienced designer, since general rules to avoid it are not available.

In crystal oscillators there is a tendency to spurious signals due to the crystal itself. For studying these effects a more complete model of the crystal with additional resonances (so-called *modes*) has to be taken into consideration [see Parzen (6)].

Another effect is self-produced amplitude modulation of the high-frequency oscillation; this effect is often called *squegging*. The physical reason for squegging is related to an interaction between the time constant of the bias and coupling circuits and the time constants of the high-frequency tuned circuits of the oscillation part. Squegging occurs more frequently in self-limiting oscillators with low $Q$'s than in crystal oscillators, where a high $Q$ is usual. Furthermore, a suitable thermal design is necessary, especially if a crystal resonator is chosen. Some hints about this subject can be found in the literature [see e.g. Kurz, and Mathis (33)].

## BIBLIOGRAPHY


1. G. Vallauri Über die Wirkungsweise der in der drahtlosen Telegraphie benutzten Vakuumröhren mit drei Elektroden (Audion), *Jahrb. Drahtlosen Telegr.*, **12** 349, 1917.
2. A. A. Andronov A. A. Vitts S. E. Khaikin *Theory of Oscillators* (reprint), New York: Dover, 1996.
3. N. M. Krylov N. N. Bogoliubov *Einführung in die Nichtlineare Mechanik*, Verlag Akad. Wiss. Ukr. SSR, 1937.
4. J. A. Sanders F. Verhulst *Averaging Methods in Nonlinear Dynamical Systems* New York: Springer, 1985.
5. W. Mathis *Theorie Nichtlinearer Netzwerke*, Berlin: Springer, 1987.
6. B. Parzen *Design of Crystal and Other Harmonic Oscillators*, New York: Wiley, 1983.
7. J. K. Hale *Oscillations in Nonlinear Systems*, New York: McGraw-Hill, 1963.
8. J. Guckenheimer Dynamics of the van der Pol equation, *IEEE Trans. Circuits Syst.* **CAS-27**: 983–989, 1980.
9. J. Millman A. Grabel *Microelectronics*, New York: McGraw-Hill, 1987.
10. K. Heegner Über Schwingungserzeugung mittels Elektronenröhren, welche Selbstinduktion nicht enthalten, *Jahrb. Drahtlosen Telegr.*, **29**: 1927, 151.
11. R. S. Sidorowicz An abundance of sinusoidal oscillators. *Proc. IEE*, **119**: 283–293, 1972.
12. D. W. Jordan P. Smith *Nonlinear Ordinary Differential Equations*, 3 ed. Oxford: Oxford University Press, 1999.
13. V. I. Arnold *Geometrical Methods in the Theory of Ordinary Differential Equations*, New York: Springer, 1983.
14. G. Nicolis I. Prigogine. *Self-Organization in Non-equilibrium Systems*, Wiley, Chichester: 1997.
15. D. K. Arrowsmith C. M. Place *An Introduction to Dynamical System*, Cambridge, UK: Cambridge University Press, 1990.
16. B. D. Hassard N. D. Kazarinoff Y.-H. Wan *Theory and Applications of Hopf Bifurcation*, Cambridge, Cambridge University Press, 1981.
17. A. I. Mees *Dynamics of Feedback Systems*, Chichester: Wiley, 1981.
18. L. A. Hazeltine Oscillating audio circuits, *Proc. Inst. Radio Engrs.* **6**: 63, 1918.
19. R. Spence *Linear Active Networks*, New York: Wiley, 1970.
20. E. J. Cassignol *Semiconductors, Vol. III. Non-linear Electronics*, Philips Techn. Library, Eindhoven, The Netherlands: N.V. Gloeilampenfabrieken, 1968.
21. C. A. Desoer E. S. Kuh *Basic Circuit Theory*, New York: McGraw-Hill, 1969.
22. R. Mauro *Engineering Electronics—a Practical Approach*, Englewood Cliffs, NJ: Prentice-Hall, 1989.

23. D. Meyer-Ebrecht Schnelle Ampitudenregelung harmonischer Oszillatoren, Dissertation, TU Braunschweig, 1974.
24. A. H. Nayfeh *Introduction to Perturbation Techniques*, New York: Wiley, 1981.
25. U. Kirchgraber E. Stiefel *Methoden der Analytischen Störungsrechnung und Ihre Anwendung*, Stuttgart: Teubner Verlag, 1978.
26. C. Keidies W. Mathis Application of symbolic methods to oscillator design, *Proc. 2nd SMACD'92 Florenz, (Italy)*, 1992, pp. 67–72.
27. R. Knöchel K. Schünemann Noise in multiple-device oscillators, *Arch. Elekktron* übertragungstech. **36** (10): 31–39, 1982.
28. A. Buonomo C. Di Bello Asymptotic formulas in nearly sinusoidal nonlinear oscillators. *IEEE Trans. Circuits Syst. I, Fundam. Theory Appl.*, **43**: 953–963, 1996.
29. V. Belevitch *Classical Network Theory*, San Francisco CA: Holden-Day, 1968.
30. T. Mangold P. Russer Full–wave modeling and automatic equivalent-circuit generation of millimeter-wave planar and multilayer structures, *IEEE Trans. Microw. Theory Tech.*, **MTT-47**: 851–858, 1999.
31. M. N. Horenstein *Microelectronic Circuits and Devices*, Englewood Cliffs, N: Prentice-Hall, 1996.
32. P. R. Gray R. G. Meyer *Analysis and Design of Analog Integrated Circuits*, New York: Wiley, 1993.
33. G. Kurz W. Mathis *Oszillatoren*, Heidelberg: Hüthig Buch Verlag, 1994.
34. J. Davidse *Analog Circuit Design*, New York: Prentice-Hall 1991.
35. T. J. Aprille T. N. Trick A computer algorithm to determine the steady state response of nonlinear oscillators, *IEEE Trans. Circuit Theory*, **19**: 131–139, 1972.
36. L. O. Chua P. Lin *Computer-Aided Analysis of Electronic Circuits: Algorithms and Computational Techniques*, Englewood Cliffs, NJ: Prentice-Hall, 1975.
37. M. Schwab, *et al.* Steady state of a SAW stabilized bipolar oscillator obtained by solution of a boundary value problem, *Proc. 20th European Microwave Conf.*, Budapest, 1990, pp. 1240–1245.
38. S. A. Maas *Nonlinear Microwave Circuits*, Norwood MA: Artech House, 1988.
39. V. Rizzoli A. Neri State of the art and present trends in nonlinear microwave CAD techniques, *IEEE Trans. Microw. Theory Tech.*, **MTT-36**: 343–364, 1988.
40. B. Roth H. Sledzik A. Beyer An improved method for the design and simulation of microwave oscillators, *Proc. West Germany IEEE MTT/AP Joint Chapter Workshop "Progress in Microwave CAD and in CAD Applications,"* Ratingen, 1989, pp. 208–224.
41. Y. Hu J. J. Obregon J.-C. Mollier Nonlinear oscillation via Volterra series, *IEEE Trans. Circuits Syst.*, **CAS-29:1** 50–168, 1982.
42. C.-R. Chang M. B. Steer Frequency-domain nonlinear microwave simulation using the arithmetic operator method, *IEEE Trans. Microw. Theory Tech.*, **MTT-38**: 1139–1143, 1990.
43. M. Schwab Determination of the steady state of an oscillator by a combined time–frequency domain method, *IEEE Trans. Microw. Theory Tech.*, **MTT-39**: 1391–1402, 1991.
44. S. K. Kundert A. Sangiovanni-Vincentelli *Steady State Methods for Simulating Analog and Microwave Circuits*, Boston: Kluwer Academic, 1990.
45. M. Filleböck M. Schwab P. Russer Automatic generation of starting values for the simulation of microwave oscillators by frequency domain techniques, *IEEE Trans. Microw. Theory Tech.*, **41**: 809–813, 1993.
46. T. Goeller M. Schwab P. Russer Efficient simulation of millimeter-wave IMPATT oscillators by FATE, a combined time- and frequency-domain method, *IEEE Microw. Guided wave Lett.*, **1**: 343–345, 1991.
47. A. Dupuis J. Hausner P. Russer Hybrid integrated Ku-band VCO, *Proc. 19th European Microwave Conf.*, London 1989, pp. 1009–1014.
48. R. Gratzl J. Hausner P. Russer Nonlinear design approach of a broadband hybrid integrated Ku-band common source GaAs FET VCO, Proc. *International Microwave Symp.*, Dallas, 1990, pp. 739–742.
49. R. Bulirsch *Die Mehrzielmethode zur Numerischen Lösung von nichtlinearen Randwert-problemen und Aufgaben der Optimalen Steuerung*, Heidelberg: Carl-Cranz-Gesellschaft, 1971; Munich: Technische Universität, Mathematisches Institut, 1985.
50. R. Bulirsch J. Stoer *Introduction to Numerical Analysis*, New York: Springer, 1980. *Differential Equations*, Englewood Cliffs N: Prentice-Hall, 1971.
51. L. Gustafson G. H. B. Hanson K. I. Lundstroem On use of the describing functions in the study of nonlinear active microwave circuits. *IEEE Trans. Micro Theory Tech.*, **MTT-20**: 402–409, 1972.

52. A. Spälti Der Einflu$\beta$ des thermischen Widerstandsrauschens und des Schroteffektes auf die Störmodulation von Oszillatoren, *Bull. Schweiz. Elektr. Vereins*, **39**: 419–427, 1948.
53. W. A. Edson Noise in oscillators, *Proc. IRE*, **48**: 1454–1466, 1960.
54. K. Kurokawa Noise in synchronized oscillators, *IEEE Trans. Microw. Theory Tech.*, **MTT-16**: 234–240, 1968.
55. K. Kurokawa Injection locking of microwave solid-state oscillators, *Proc. IEEE*, **61**: 1386–1408, 1973.
56. K. F. Schünemann K. Behm Nonlinear noise theory for synchronized oscillators, *IEEE Trans. Microw. Theory Tech.*, **MTT-27**: 452–458, 1979.
57. L. O. Chua Y.-S. Tang Nonlinear oscillation via Volterra series, *IEEE Trans. Circuits Syst.*, **CAS-29**: 150–168, 1982.
58. K. März Phasen- und Amplitudenschwankungen in Oszillatoren, *Arch Elektron.* Übertragungstech. **24** (11): 477–490, 1970.
59. F. X. Kärtner Determination of the correlation spectrum of oscillators with low noise, *IEEE Trans. Microw. Theory Tech.*, **MTT-37**: 90–101, 1989.
60. F. X. Kärtner Analysis of white and $f^{-\alpha}$ noise in oscillators, *Int. J. Circuit Theory Appl.* **18**: 485–519, 1990.
61. V. Güngerich *et al.* Phase noise reduction of microwave oscillators by optimization of the dynamic behaviour, *MTT-S International Microwave Symp. 1994*, San Diego, 1994, pp. 953–956.
62. G. R. Olbrich *et al.* Calculation of HEMT oscillator phase noise using large signal analysis in time domain, *IEEE-MTT Symp. Digest*, San Diego, Vol. 2, pp. 965–968. 1994.
63. V. Güngerich *et al.* Reduced phase noise of a varactor tunable oscillator: Numerical calculations and experimental results. *IEEE MTT-S International Microwave Symp.* 1993 Atlanta, 1993, pp. 561–564.
64. W. Anzill F. X. Kärtner P. Russer Simulation of the single sideband phase noise of oscillators, *Second International Workshop of the German IEEE MTT/AP Joint Chapter on Integrated Nonlinear Microwave and Millimeterwave Circuits*, Duisburg, Germany 1992, pp. 97–110.
65. W. Anzill P. Russer A general method based on harmonic balance techniques to simulate noise in free running oscillators, *IEEE MTT-S International microwave Symp. 1993*, Atlanta, GA), 1993, pp. 655–658.
66. W. Anzill P. Russer A general method to simulate noise in oscillators based on frequency domain techniques, *IEEE Trans. Microw. Theory Tech.*, **41**, 2256–2263, 1993.
67. H. Hillbrand P. Russer An efficient method for computer aided noise analysis of linear amplifier networks, *IEEE Trans. Circuits and Syst.* **CAS-23**: 235–238, 1976.
68. P. Russer H. Hillbrand Rauschanalyse von linearen Netzwerken, *Wiss. Beri. AEG-Telefunken*, **49**: 127–138, 1976.
69. W. Anzill Berechnung und Optimierung des Phasenrauschens von Oszillatoren, Dis sertation, Technische Universität München, 1995.
70. W. Anzill *et al.* Phase noise minimization of microwave oscillators by optimal control, *IEEE MTT-S International Microwave Symp.*, 1995, (Orlando, FL, pp. 1565–1568.
71. A. Rusznyak Start-up time of CMOS oscillators, *IEEE Trans. Circuits Syst.* **CAS-34**: 259–268, 1987.
72. C. Schmidt-Kreusel Rechnergestützte Analyse von Quarzoszillatoren, Dissertation, University of Wuppertal, 1997.
73. W. Mathis An efficient method for the transient analysis of weakly damped crystal oscillators, *Proc. MTNS98*, Padova, Italy, 1998.
74. H. G. Brachtendorf Laur. R. Multi-rate PDE methods for high $Q$ oscillators *Proc. 4th Circuits, Systems, Communications & Computers (CSCC) 2000*, Athens, 2000.
75. W. B. Davenport W. L. Root *An Introduction to the Theory of Random Signals and Noise*, New York: McGraw-Hill, 1958.
76. J. H. Wilkinson *The Algebraic Eigenvalue Problem*, Oxford: Clarendon, 1988.
77. G. H. Golub C. T. Van Loan *Matrix Computations*, Baltimore: Johns Hopkins University Press, 1989.
78. F. X. Kärtner Noise in oscillating systems, *Proc. IEEE MTT/AP Workshop on Integrated Nonlinear Microwave and Millimeter Wave Circuits (INMIC'92)*, Duisburg, Germany, 1992, pp. 61–75.
79. W. Anzill F. X. Kärtner P. Russer Simulation of the phase noise of oscillators in the frequency domain, *Arch. Elek. Ubertragung., AE* **48**(1): 45–50, 1994.
80. H. G. Möller Über störungsfreien Gleichstromempfang mit dem Schwingaudion, *Jahrb. Drahtl. Telegr.*, **17**: 256, 1921.
81. B. L. Van der Pol Forced oscillations in a circuit with nonlinear resistance (reception with reactive triode), *Phil. Mag.*, **3**: 65–80, 1927. (First published in the Dutch journal *Tijdschr. Nederlandsch Radiogenootschap* in 1924.
82. E. V. Appleton The automatic synchronization of triode oscillators, *Proc. Cambridge Phil. Soc.*, **21**: 231, 1922.
83. B. L. Van der Pol The nonlinear theory of electrical oscillations, *Proc. Inst. Radio Eng. (IRE)*, **22**: 1051–1086, 1934.
84. A. A. Andronov A. A. Vitt Theorie des Mitnehmens von van der Pol. *Arch. Elektrotechn.* **24**: 99–110, 1930.

85. D. G. Tucker Forced oscillations in oscillator circuits, and the synchronization of oscillators. *J. IEE*, **92**: 226–234, 1945.
86. F. Kirschstein Die Mitnahme selbsterregter Schwingungen und ihre technische Verwertung, *Elektr. Nachr.* **20**: 29–38, 1943.
87. J. L. Stensby *Phase-Locked Loops–-Theory and Applications*, Boca Raton, FL: CRC Press, 1997.
88. Y. S. Tsang A. I. Mees L. O. Chua Synchronization and chaos, *IEEE Trans. Circuits Syst.*, **CAS-30**: 620–626, 1983.
89. M. E. Frerking *Crystal Oscillator Design and Temperature Compensation*, Van Nostrand Reinhold, New York: 1978.
90. G. D. Vendelin *Microwave Circuit Design Using Linear and Nonlinear Techniques*, New York: Wiley, 1990.

WOLFGANG MATHIS
PETER RUSSER
Otto von Guericke University of Magdeburg